ORNL/SPR-2022/2643

Second group of irradiation capsules: property data of irradiated welded stainless steel 347 and irradiated, welded, and hydrogen charged Zircaloy-4 for SHINE

Lauren Garrison
John Echols
Nathan Reid
Jordan Reed
Xiang Chen

September 2022

OAK RIDGE National Laboratory

ORNL IS MANAGED BY UT-BATTELLE LLC FOR THE US DEPARTMENT OF ENERGY

ORNL/SPR-2022/2643

Material Science and Technology Division

SECOND GROUP OF IRRADIATION CAPSULES: PROPERTY DATA OF IRRADIATED WELDED STAINLESS STEEL 347 AND IRRADIATED, WELDED, AND HYDROGEN CHARGED ZIRCALOY-4 FOR SHINE

Lauren Garrison
John Echols
Nathan Reid
Jordan Reed
Xiang Chen

September 2022

Prepared by
OAK RIDGE NATIONAL LABORATORY
Oak Ridge, TN 37831-6283
managed by
UT-BATTELLE LLC
for the
US DEPARTMENT OF ENERGY
under contract DE-AC05-00OR22725

ACKNOWLEDGMENTS
Support for this research was provided by the US Department of Energy's National Nuclear Security Administration (DOE/NNSA), Office of Material Management and Minimization, Molybdenum-99 Program. The authors would also like to thank the following coworkers for their contributions to completing this research project: Adrian Schrell, Cade Abbott, and Eric Manneschmidt.

CONTENTS

ABSTRACT

Zircaloy-4 and AISI 347 stainless steel were irradiated to low doses (10^{20} and 10^{21} n/cm^2) at low temperature (~60°C) in the High Flux Isotope Reactor (HFIR) at Oak Ridge National Laboratory (ORNL). These materials were under consideration for some of the structural components of the medical isotope production facility developed by SHINE Technologies. Zircaloy-4 base metal, as welded, welded and post-weld heat treated (PWHT), and hydrogen charged samples were irradiated. AISI 347 base metal from Sandmeyer Steel, Penn Stainless, and Rolled Alloys suppliers were irradiated. AISI 347 gas tungsten arc welding (GTAW) and flux-cored arc welding (FCAW) samples of Penn Stainless and Rolled Alloys were also irradiated. The irradiated materials were tested with microhardness and tensile tests at room temperature in air. The AISI 347 materials had more elongation after irradiation than the Zircaloy-4 materials. In fact, the Zircaloy-4 welded without PWHT and with H charging had the lowest elongation of any of the materials. This report is the final in a series of reports on this project.

1. INTRODUCTION

This project has investigated irradiated properties of structural materials for the Target Solution Vessel (TSV) and connected pipes for SHINE Technologies through the US Department of Energy's National Nuclear Security Administration (DOE/NNSA), Office of Material Management and Minimization, Molybdenum-99 Program. Initially Zircaloy-4 was investigated, but more recently the focus turned to AISI 347. This report is the final in a series of reports in the collaboration with SHINE. Some brief highlights of each of the relevant reports in this series are listed below. The other reports will be referenced throughout this report, but more thorough descriptions can be found in their original text.

- "Evaluation of Zircaloy-4 as the structural material for the Target Solution Vessel and support lines of SHINE — Sample preparation for the third-round neutron irradiation" ORNL/TM-2017/482 (Ref. [1])
    - This report included hydrogen charging and welding of Zircaloy-4. The H charged material was investigated with EBSD pole figure texture, XRD, and SEM. Tensile tests were completed on the welded and H charged material. Post weld heat treatment (PWHT) at select different temperatures and times were completed and tensile tests done on the material after PWHT. The differences between symmetric cut and asymmetric cut tensile samples from the weld region was investigated. All tensile data reported in this report is raw and has not been analyzed to remove the machine compliance.
- "Evaluation of Zircaloy-4 Welding and Hydrogen Charging Effects for Use as the Structural Material for the Target Solution Vessel and Support Lines of SHINE" ORNL/TM-2018/1035 (Ref. [2])
    - The data from 800°C PWHT on zircaloy was re-analyzed to remove machine compliance, and additional tests were done on 800°C 1 h. Two strain rates for the tensile tests were compared. Microhardness was performed. One H charging test was done.
- "Zircaloy-4 and Stainless Steel 347 Property Data and Microstructures Related to the Structural Material for the Target Solution Vessel and Support Lines of SHINE" ORNL/SPR-2019/1356 (Ref. [3])
    - This is the first report that investigated AISI 347, so contains background information on the alloy and summary of data available in the literature. Characterization was done of microstructure, elemental composition, and tensile properties of the AISI 347 plates obtained from three suppliers. The Zircaoloy-4 post-weld heat treated samples were analyzed in greater detail, building on initial results in the first two reports.
- "Welded and Hydrogen Charged Zircaloy-4 and Welded Stainless Steel 347 Property Data and Microstructures for the Target Solution Vessel and Support Lines of SHINE" ORNL/SPR-2020/1879 (Ref. [4])

  - Zircaloy-4 samples were hydrogen charged and tensile tested. The optimal PWHT for elongation was determined to be 800°C 1 h. AISI 347 from two suppliers were welded using both gas tungsten arc welding (GTAW) and flux-cored arc welding (FCAW). The welding procedure is described in detail. Tensile properties of asymmetric and symmetric samples from the weld bars were obtained. An alternative to a full AISI 347 TSV, a thin layer of AISI 347 was explosion welded on to a low alloy steel substrate (alloy SA-516-70N). Initial tensile and microstructure investigations were completed on the clad material. The first group of four capsules containing Zircaloy-4 and AISI 347 were irradiated.
- "Property data of irradiated SS 347 and irradiated, welded, and hydrogen charged Zircaloy-4 for the target solution vessel and support lines of SHINE" ORNL/SPR-2021/2397 (Ref. [5])
  - Microhardness and tensile properties of the first group of four irradiation capsules were reported. Charpy impact testing was completed on unirradiated AISI 347 from the three suppliers. More detail on the microstructure, phases, and tensile properties of the clad material was presented.

The present report focuses on the results from the second group of four irradiation capsules, which included hydrogen charged and welded Zircaloy-4, welded AISI 347, and AISI 347 clad onto an SA-516-70 substrate. These materials were microhardness and tensile tested.

2. EXPERIMENTAL METHODS

2.1 MATERIAL INFORMATION

2.1.1 AISI 347

The full description of the as-received AISI 347 materials is covered in report ORNL/SPR-2019/1356 [3]. AISI 347 was purchased from Penn Stainless, Rolled Alloys and Sandmeyer Steel. Each material met the ASTM A240 standards for composition (Table 1) and mechanical properties, but each had slight variations. Notably, the Rolled Alloys material had the highest Mo impurity at 0.3 wt % while Penn Stainless had the lowest at 0.029 wt.%. The as-received, unirradiated microstructure (Figure 1) and phases (Figure 2) are reprinted here from Ref. [3]. The Rolled Alloys material has the largest grains and the most proportion of FCC phase. The Penn Stainless has the smallest average grain size and the highest proportion of BCC phase of the three materials. Each of the three plates were machined into tensile samples with two perpendicular orientations, called A and B (Figure 3). It was determined from the texture analysis that the A direction was the rolling direction for Penn Stainless, but the texture analysis was inconclusive for Rolled Alloys and Sandmeyer, so the labeling convention A and B was kept throughout the experiments. The EBSD data for grain sizes in the A and B directions were plotted in Figure 4. Penn Stainless tensile bars in A and B orientations were irradiated, whereas Rolled Alloys and Sandmeyer Steel samples were only irradiated in the A orientation.

Table 1. Chemical composition of AISI 347 from different suppliers. All values are given in percent by weight. Table reproduced from Ref. [3].

		Suppliers			
Technique	**Elements**	**Penn Stainless**	**Rolled Alloys**	**Sandmeyer**	**ASTM A240**
ICP-OES	Fe	Balance	Balance	Balance	Balance
	Cr	17.3 (wt%)	17.5 (wt%)	17.8 (wt%)	17-19 (wt%)
	Mn	1.42	1.17	1.1	2

	Ni	9.28	9.75	9.64	9-13
	Si	0.36	0.77	0.7	0.75
IGA	C	0.045	0.046	0.053	0.08
	O	0.0020	0.0016	0.0045	N/A
	S	0.0012	0.00075	0.0015	0.030
GDOES	P	0.025	0.029	0.027	0.45
	Nb	0.2	0.3	0.3	10×C
	Si	0.36	0.77	0.7	0.75
	Co	0.023	0.1	0.3	N/A
	Cu	0.022	0.3	0.1	N/A
	Mo	0.029	0.3	0.15	N/A
	V	0.012	0.056	0.059	N/A

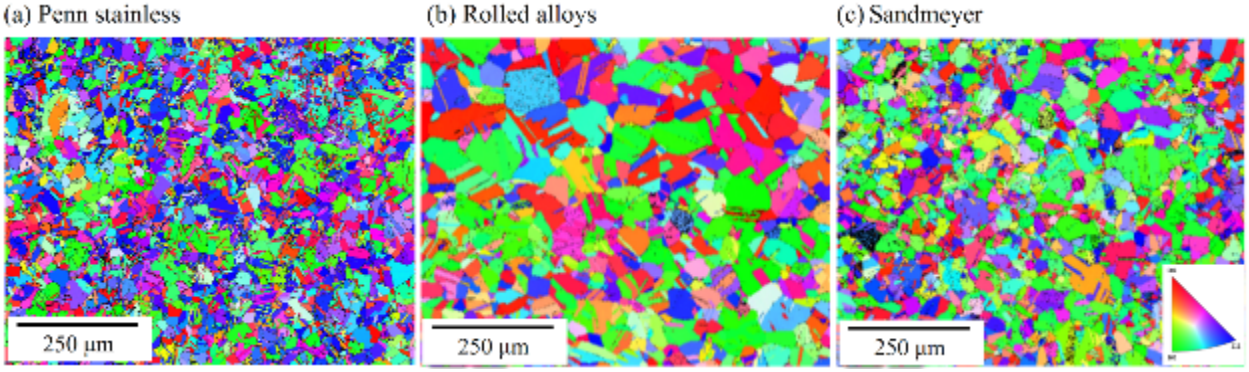

Figure 1. EBSD inverse pole figure maps of AISI 347 supplied by: (a) Penn stainless, (b) Rolled alloys, and (c) Sandmeyer. Direction A is vertical, and B is horizontal. Figure reproduced from [3].

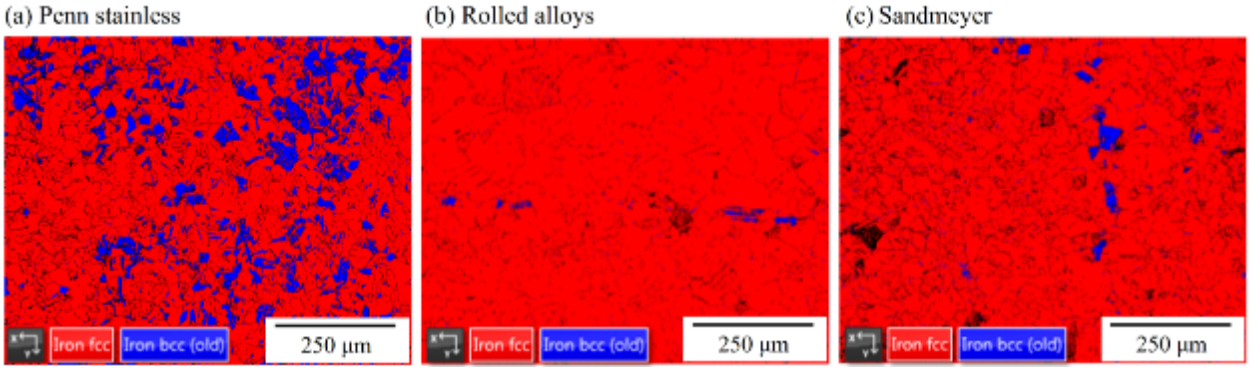

Figure 2. EBSD phase maps of AISI 347 supplied by: (a) Penn stainless, (b) Rolled alloys, and (c) Sandmeyer. Figure reproduced from [3].

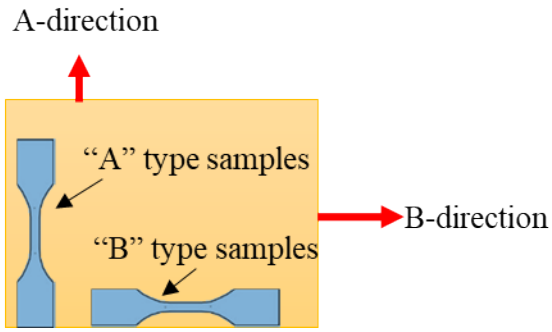

Figure 3. Tensile samples were cut in perpendicular directions A and B. Figure reproduced from [3].

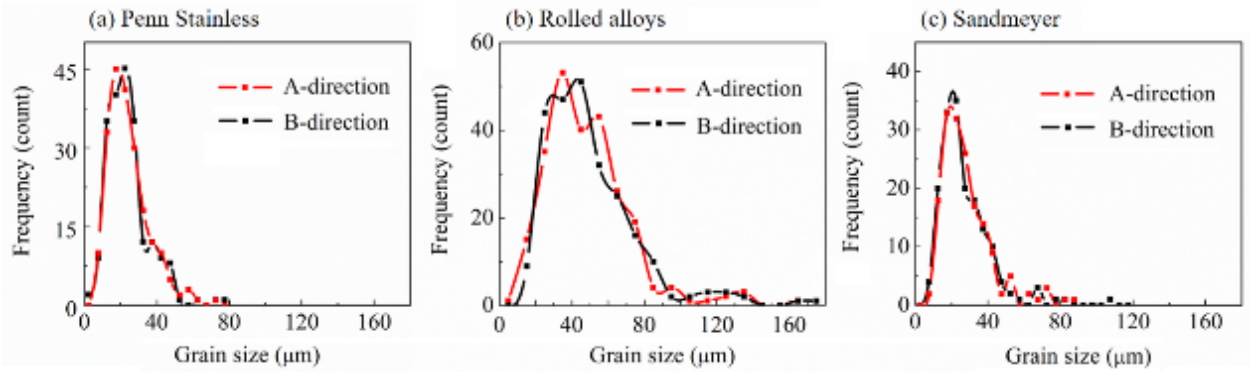

Figure 4. Grain size distribution along A and B directions for AISI 347 supplied by: (a) Penn stainless, (b) Rolled alloys, and (c) Sandmeyer. Figure reproduced from [3].

Welding trials were conducted on Rolled Alloys and Penn Stainless produced material. They were selected because they had the most difference in terms of grain size and impurity content. In the SHINE system both FCAW and GTAW type welds will be used in different locations based on the thickness of the material, so both were tested here. The geometries of the test bars are shown in Figure 5. The GTAW bar is the same geometry as was used previously for the Zircaloy-4 welding trials. The details of the welding procedure and results are in Report ORNL/SPR-2020/1879 [4].

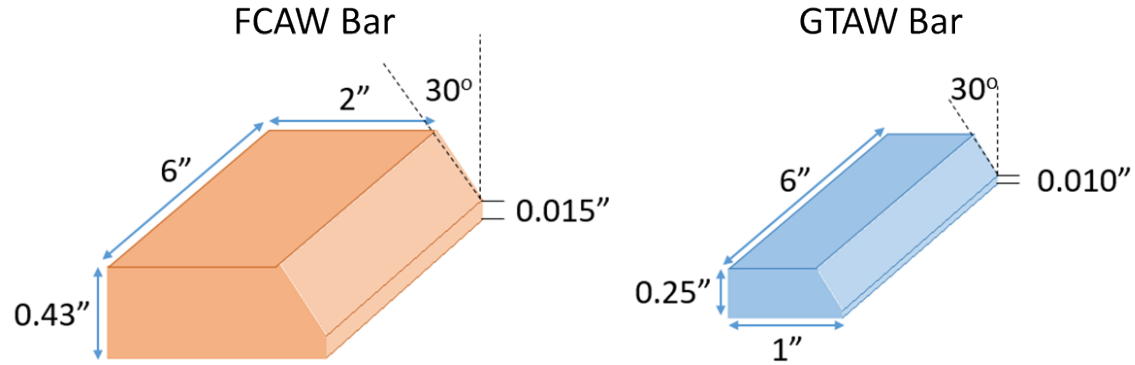

Figure 5. Weld bar geometries for the FCAW and GTAW type of welds are shown. For each weld trial, two FCAW or two GTAW bars and corresponding filler material are necessary for complete welds. Figure is reproduced from [4].

Figure 6 shows the layout of samples machined from the welded bars. The asymmetric samples behaved similarly to the base metal because the fusion zone and heat affected zones are not in the region of the tensile gauge section that experiences the most strain [4]. Only symmetric samples were included in the irradiation because they show the most impact of the weld. The tensile axis of the tensile samples cut from the welded bars is the B orientation as described in Figure 3. Thus for Penn Stainless the tensile bars from the welded coupons are perpendicular to the rolling direction, but for Rolled Alloys the mechanical behavior was very similar in the A and B directions and neither could be declared the rolling direction [3]. Because the welded bars used a V shape between the two halves of the coupon, there is more filler and a thicker weld at the top of the weld versus the root side. Thus, the layer of tensile samples cut from the welded bars was tracked as the samples were machined (Figure 6b).

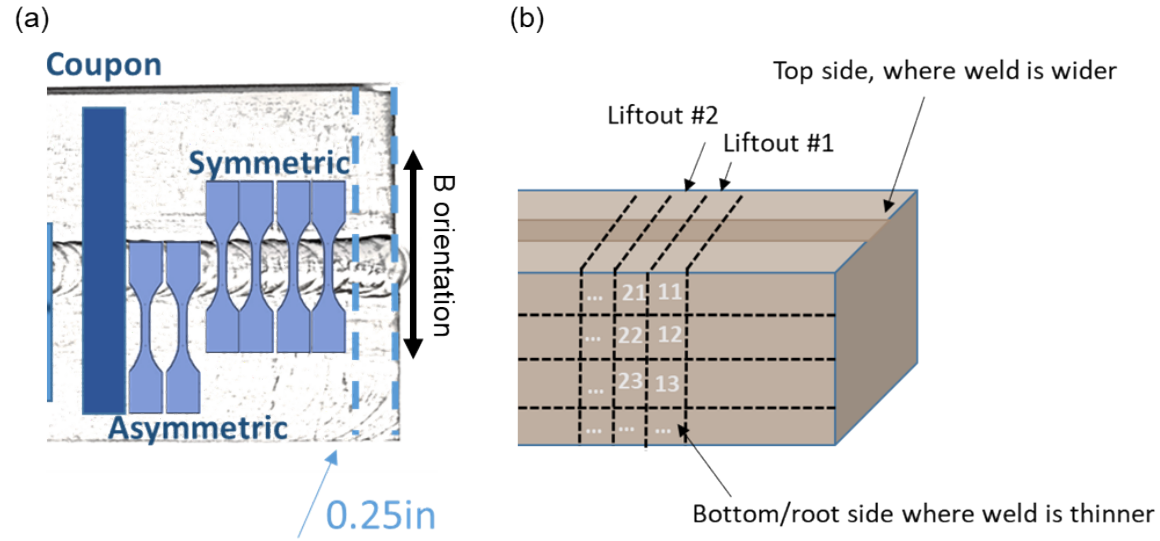

Figure 6. (a) Illustration of how samples were machined relative to the weld seam. The tensile direction of the samples cut from the weld bars matches the "B" orientation of the base metal plates as defined above. A GTAW weld bar geometry is shown but the same layout was used for the FCAW bars. (b) Sample identification numbers included two numeric digits to track the lift out and layer from which the sample was machined. Reproduced from [4].

2.1.2 Explosion Welded Plate

Stainless steel is needed as a corrosion barrier in aqueous systems like the SHINE facility, but the downside is that it is more expensive and higher activity after neutron irradiation as compared to a low alloy steel. As an alternative to complete AISI 347 components, a thin layer of AISI 347 bonded to a low alloy steel plate was investigated. This clad plate was produced by NobleClad by explosively welding a ~1 mm thick AISI 347 layer onto a 51 mm thick alloy SA-516-70N base metal. The interface between the cladding and the base plate has a wavy shape [4]. Samples of the explosion welded plate were included in the irradiation capsules. These samples were machined such that the interface between the AISI 347 and the base metal was approximately at the center as in Figure 7.

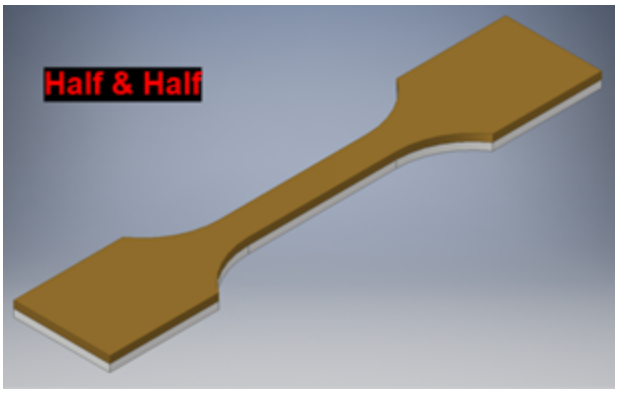

Figure 7. Rendering of the type of explosion welded plate included in the irradiation that has approximately half AISI 347 (brown color in image) and half alloy SA-516-70N (light grey). Reproduced from [4].

2.1.3 Zircaloy-4

The Zircaloy-4 used in this project was produced by ATI Specialty Alloys and Components, Oregon, USA in batch no. MIL-1526608. The composition was Zr, 1.54 Sn, 0.21 Fe, and 0.11 Cr in wt % with a 0.14 wt % O impurity, and ppm levels of other impurities of Al, C, N, Si, and H [1, 2]. The welded bars of Zircaloy-4 used the same dimensions as the AISI 347 GTAW bars in Figure 5. For the irradiated samples with a PWHT, 600°C for 1 h was used. It was determined that 800°C 1 h may give slightly better elongation recovery, but the 600°C 1 h gave more consistent tensile results and had a temperature and time savings for only a small penalty in elongation. Thus, the 600°C was determined to be the best compromise of the different factors.

Hydrogen charging of samples was accomplished using a titanium hydride powder vacuum sealed in glass tubes with the Zircaloy-4 samples and heated in a furnace. The details are described in Report ORNL/SPR-2020/1879 [4]. After hydrogen charging, one sample from each glass tube was destructively analyzed for H content and that value was assumed to be identical to the H content in the other tensile bars charged in the same tube.

2.2 IRRADIATION

In the list below it is noted which of the materials were included in the group 1 irradiation capsules (SHINE-11, -12, -13, and -14) and were discussed in detail in Ref. [5], and which were included in group 2 capsules (SHINE-21, -22, -23, and -24) and their details are in this report. Comparisons between the two sets of results are also included here. Capsules SHINE-21 and -23 were irradiated to approximately 1.3E20 n/cm^2 while SHINE-22 and -24 were irradiated to approximately one order of magnitude higher fluence, with details of the irradiation in Table 2. The overview of the types of samples included in the irradiations are in the list below and the details of the samples in group 2 are listed in Table 3.

- Zircaloy-4
    - Group 1: SHINE-11, -12
        - Base metal
        - Base metal with low (~200 ppm H) hydrogen charging
        - As-welded (no PWHT)
        - Welded and PWHT
    - Group 2: SHINE-21, -22
        - Base metal with high (~500 ppm H) hydrogen charging

        - As-welded (no PWHT) with low (~200) or high (~400 ppm H) hydrogen charging
        - Welded and PWHT with low (~200) or high (~400 ppm H) hydrogen charging
- AISI 347
    - Group 1: SHINE-13, -14
        - Rolled Alloys produced AISI 347 base metal
        - Penn Stainless produced AISI 347 base metal in two orientations
        - Sandmeyer Steel produced AISI 347 base metal
    - Group 2: SHINE-23, -24
        - Rolled Alloys produced AISI 347 welded by GTAW or FCAW
        - Penn Stainless produced AISI 347 welded by GTAW or FCAW
        - Explosion welded AISI 347 layer on SA-516-70 substrate, machined so the interface is at the center of the sample

Table 2 shows the details of the irradiation of the group 2 capsules. All four capsules were irradiated in the hydraulic tube of the High Flux Isotope Reactor (HFIR). The hydraulic tube is used to irradiate capsules for less than one full cycle, which would be approximately 25 days. To achieve the desired fluences for this project irradiations of approximately 32 and 366 hours were needed (~1.3 and 15 days). HFIR has a parabolic flux profile with the highest flux at the center of the reactor and a decreased flux at the top and bottom. Thus, while capsules SHINE-22 and -24 received the same number of hours of irradiation, they were in different vertical positions in the core, so received slightly different neutron fluences. These two capsules were also irradiated partially in cycle 490C, removed from the reactor, and reinserted to finish irradiation during cycle 491. This was done to make use of the available irradiation positions in HFIR and is not expected to affect the results in any noticeable way, especially since the irradiations were performed at the coolant temperature of ~60°C so there was not a drastic temperature swing during the break between cycles.

Table 2. Irradiation details of the group 2 capsules. The location and position refer to where they were placed in the HFIR during irradiation according to the numbering system used at HFIR.

Capsule	SHINE-21	SHINE-22	SHINE-23	SHINE-24
Start Date	3/19/2021	3/22/2021	3/21/2021	3/22/2021
Start Time	16:34	22:07	0:40	3:04
End Date	3/21/2021	4/24/2021	3/22/3021	4/24/2021
End Time	0:00	11:00	8:10	11:00
Cycle (s)	490C	490C and 491	490C	490C and 491
Total Time (h)	33.433	365.6	31.5	365.6
Seconds	120359	1316160	113400	1316160
Location	B3	B3	B3	B3
Position	6	3	6	7
Flux (n/cm^{2}s E>0.1 MeV)	1.12E+15	9.79E+14	1.12E+15	1.00E+15
Fluence (n/cm^2 E>0.1 MeV)	1.35E+20	1.29E+21	1.27E+20	1.32E+21

*Table 3. List of all samples irradiated in this segment of the project. Two similar (duplicates where possible) samples of each type were irradiated. Abbreviations in the Material Type column: R=Rolled Alloys; P=Penn Stainless; BM=base metal; GTAW=gas tungsten arc welded; FCAW=flux core arc welded; GTAW-P=welded and post weld heat treated with 5 h ramp and 1 h hold at 600°C; EW=explosion welded; *=samples that were microhardness tested in a row along the full length of the sample, all other samples were hardness tested only in the tensile tab regions.*

Capsule ID	Fluence (n/cm^2)	Sample ID	Material Type
SHINE-21	1.35E20	Z-108	Zry-4 BM; 470 ppm H
SHINE-21	1.35E20	Z-112	Zry-4 BM; 510 ppm H
SHINE-21	1.35E20	ZO-07	Zry-4 GTAW; 200 ppm H
SHINE-21	1.35E20	ZO-08	Zry-4 GTAW; 200 ppm H
SHINE-21	1.35E20	ZO-17	Zry-4 GTAW; 380 ppm H
SHINE-21	1.35E20	ZO-19	Zry-4 GTAW; 380 ppm H
SHINE-21	1.35E20	ZN-09	Zry-4 GTAW-P; 200 ppm H
SHINE-21	1.35E20	ZN-11	Zry-4 GTAW-P; 200 ppm H
SHINE-21	1.35E20	ZN-18	Zry-4 GTAW-P; 400 ppm H
SHINE-21	1.35E20	ZN-20	Zry-4 GTAW-P; 400 ppm H
SHINE-22	1.29E21	Z-111	Zry-4 BM; 470 ppm H
SHINE-22	1.29E21	Z-113	Zry-4 BM; 510 ppm H
SHINE-22	1.29E21	ZO-13	Zry-4 GTAW; 200 ppm H
SHINE-22	1.29E21	ZO-14	Zry-4 GTAW; 200 ppm H
SHINE-22	1.29E21	ZO-27	Zry-4 GTAW; 380 ppm H
SHINE-22	1.29E21	ZO-28	Zry-4 GTAW; 380 ppm H
SHINE-22	1.29E21	ZN-14	Zry-4 GTAW-P; 180 ppm H
SHINE-22	1.29E21	ZN-16	Zry-4 GTAW-P; 180 ppm H
SHINE-22	1.29E21	ZN-22	Zry-4 GTAW-P; 390 ppm H
SHINE-22	1.29E21	ZN-23	Zry-4 GTAW-P; 390 ppm H
SHINE-23	1.27E20	RTS-21	R AISI 347 GTAW
SHINE-23	1.27E20	RTS-23	R AISI 347 GTAW
SHINE-23	1.27E20	RFS-21	R AISI 347 FCAW
SHINE-23	1.27E20	RFS-25	R AISI 347 FCAW
SHINE-23	1.27E20	RFS-11	R AISI 347 FCAW
SHINE-23	1.27E20	PTS-11	P AISI 347 GTAW
SHINE-23	1.27E20	PTS-13	P AISI 347 GTAW
SHINE-23	1.27E20	PFS-11	P AISI 347 FCAW
SHINE-23	1.27E20	PFS-15	P AISI 347 FCAW
SHINE-23	1.27E20	PFS-41	P AISI 347 FCAW
SHINE-23	1.27E20	FC/FB-1	EW; half AISI 347 half SA-516-70
SHINE-23	1.27E20	FC/FB-3	EW; half AISI 347 half SA-516-70
SHINE-24	1.32E21	RTS-31	R AISI 347 GTAW
SHINE-24	1.32E21	RTS-33	R AISI 347 GTAW
SHINE-24	1.32E21	RFS-31	R AISI 347 FCAW
SHINE-24	1.32E21	RFS-35*	R AISI 347 FCAW
SHINE-24	1.32E21	RFS-45	R AISI 347 FCAW
SHINE-24	1.32E21	PTS-31	P AISI 347 GTAW
SHINE-24	1.32E21	PTS-33	P AISI 347 GTAW
SHINE-24	1.32E21	PFS-35*	P AISI 347 FCAW
SHINE-24	1.32E21	PFS-21	P AISI 347 FCAW
SHINE-24	1.32E21	PFS-25	P AISI 347 FCAW
SHINE-24	1.32E21	FC/FB-4	EW; half AISI 347 half SA-516-70
SHINE-24	1.32E21	FC/FB-5	EW; half AISI 347 half SA-516-70

The irradiation capsules were the perforated type (Figure 8). The outer capsule is perforated with holes to allow the coolant water, which is 60°C, to flow through and contact the samples. The samples are not rigidly held in place and in this project a maximum of 12 samples were loaded in each capsule to ensure that there would be space for water to flow between them. The irradiation temperature of all the materials is thus taken to be 60°C. The capsules were engraved on the outer cylinder with the capsule number, as shown for SHINE-21 in Figure 9. The sample geometry used for all samples was the SS-3 type (Figure 10) which are 25.4 mm (1") long and 0.75 mm thick. The base material of the explosion welded samples, SA-516-70, has poor corrosion resistance in water. Each of those samples was wrapped in an aluminum foil envelope to prevent the samples from coming in direct contact with the HFIR coolant water during irradiation. This prevented any major corrosion damage to the samples, but after irradiation it was determined that the aluminum packets did not fully protect the samples from water and a surface discoloration was observed after irradiation.

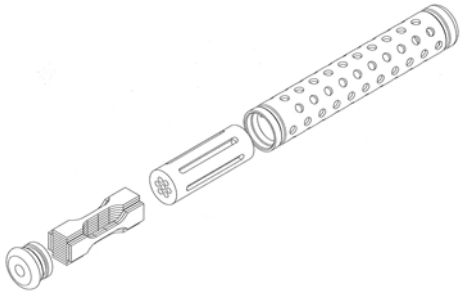

Figure 8. Exploded view of the perforated capsule with tensile samples. For scale, the tensile samples are 25.4 mm long.

Figure 9. Picture of the engraving on capsule SHINE-21.

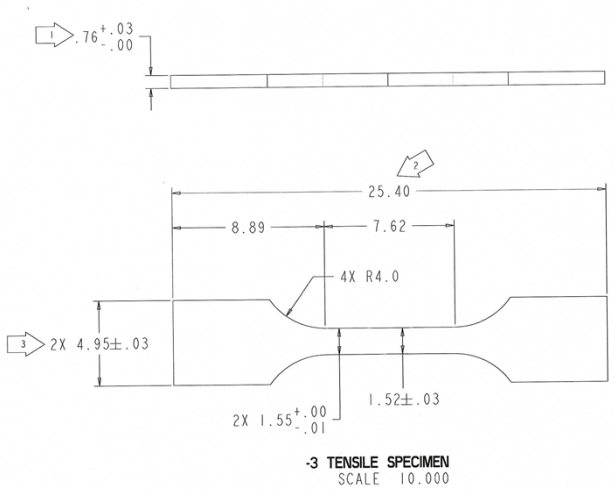

Figure 10. Dimensions of the SS-3 type tensile specimens used in this project.

2.3 MECHANICAL TESTING METHODS

2.3.1 Microhardness

Tensile shaped samples were used for all tests, so where possible microhardness indents were performed in the tab region before the samples were tensile tested. In select cases for the welded samples, microhardness indents were completed in two lines along the tensile axis of the sample to capture any difference in the fusion and heat affected zones compared to the base metal. Samples that were microhardness tested in this way through the gauge section were not used for tensile tests because the hardness indents could affect the tensile results. The unirradiated materials were Vickers microhardness tested in the tab region with a Future-Tech Corp. FM-700 digital microhardness tester. A Wilson VH3100 microhardness tester with Buehler DiaMet software was used for the programmed lines of indentations. The irradiated samples were tested in the Irradiation Material Evaluation and Testing (IMET) facility at the 3025E hot cells at ORNL. The microhardness tab indents and lines of indents (illustrated in Figure 11) were performed with the same instrument in Cell 4 of the hot cells. In all cases, 0.5 kg indent force and 10 s dwell time was used, and at least 3 indent widths of space was maintained between neighboring indents or the edge of the sample.

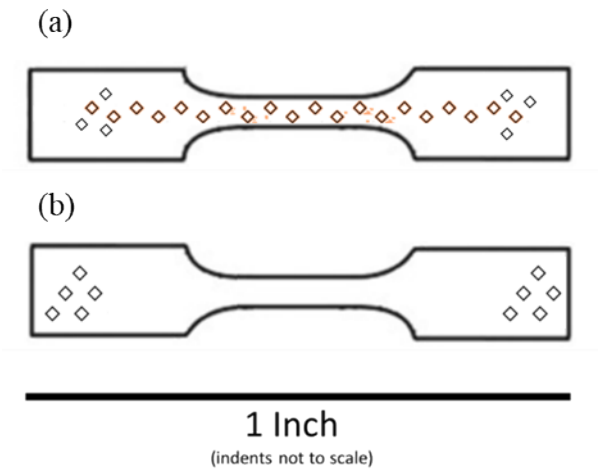

Figure 11. Illustration of the microhardness indent placement for (a) a welded sample where indents are performed in the tab region and in two lines along the tensile axis and (b) a sample that will be used for a tensile test where indents are performed in the tab region as far from the gauge section as possible.

2.3.2 Tensile Tests

All tensile tests used the SS3 geometry (Figure 10), an extension rate of 0.0003 in/s (0.00762 mm/s), and an acquisition rate of 10 Hz. The unirradiated tests were performed on the clean (non-radiological) MTS instrument in the Low Activation Materials Development and Analysis (LAMDA) laboratory, and the irradiated materials were tested on the cell 1 Instron frame with a 5 kN load cell at the IMET. All tensile tests were performed at room temperature in air. The tests did not use strain gauges and instead a data analysis program was used to remove the machine compliance from the data, as used previously and explained in Ref. [6]. After the data analysis, the stress values, uniform elongation, and total elongation are accurate. The only piece of information that cannot be recovered is the Young's Modulus, but there is not anticipated to be any significant change to it at these irradiation conditions and it is not critical for the SHINE design.

3. RESULTS

The results of the materials irradiated in the second group of irradiation capsules are presented and compared to the relevant materials from the first group of capsules and the unirradiated material. In the figure legends, the irradiation fluence is often rounded to the nearest order of magnitude (10^{20} or 10^{21} n/cm^2) and the detailed fluence for each capsule is listed in Table 3.

3.1 AISI 347 ALLOY

3.1.1 Hardness Tests

Out of the three AISI 347 suppliers, Penn Stainless and Rolled Alloys were selected for the welding trials with GTAW and FCAW type welds and were included in the group 2 irradiation capsules. The details of the microhardness values are in the Appendix Table 4. In Figure 12 the columns of graphs are labeled as base metal, GTAW, and FCAW based on what type of sample the data was taken from. However, all these data points were taken from the tab regions of the samples, so should represent the base metal even where a GTAW or FCAW sample was tested because the heat affected zone does not reach to the end of the tab region of the tensile bars. There are slight differences between the Penn Stainless base metal, GTAW, and FCAW microhardness values for the same dose, and the same is true for the Rolled Alloys samples. For example, the unirradiated Penn Stainless FCAW microhardness is slightly higher than the GTAW or base metal microhardness. The natural spread in the data is most likely what causes this. For the irradiated samples, the base metal samples were irradiated in different capsules than the welded samples, but the irradiation conditions of group 1 and 2 capsules were extremely similar. The base metal samples were irradiated in capsules SHINE-13 and -14 which received 1.29E20 and 1.32E21 n/cm^2 respectively, compared to the capsules that contained the welded samples, SHINE-23 and -24 with 1.27E20 and 1.32E21 n/cm^2 respectively. Thus, any slight differences in the hardness between the base metal and welded samples irradiated to the same fluence can be attributed to the distribution of data points and not any difference in irradiation conditions.

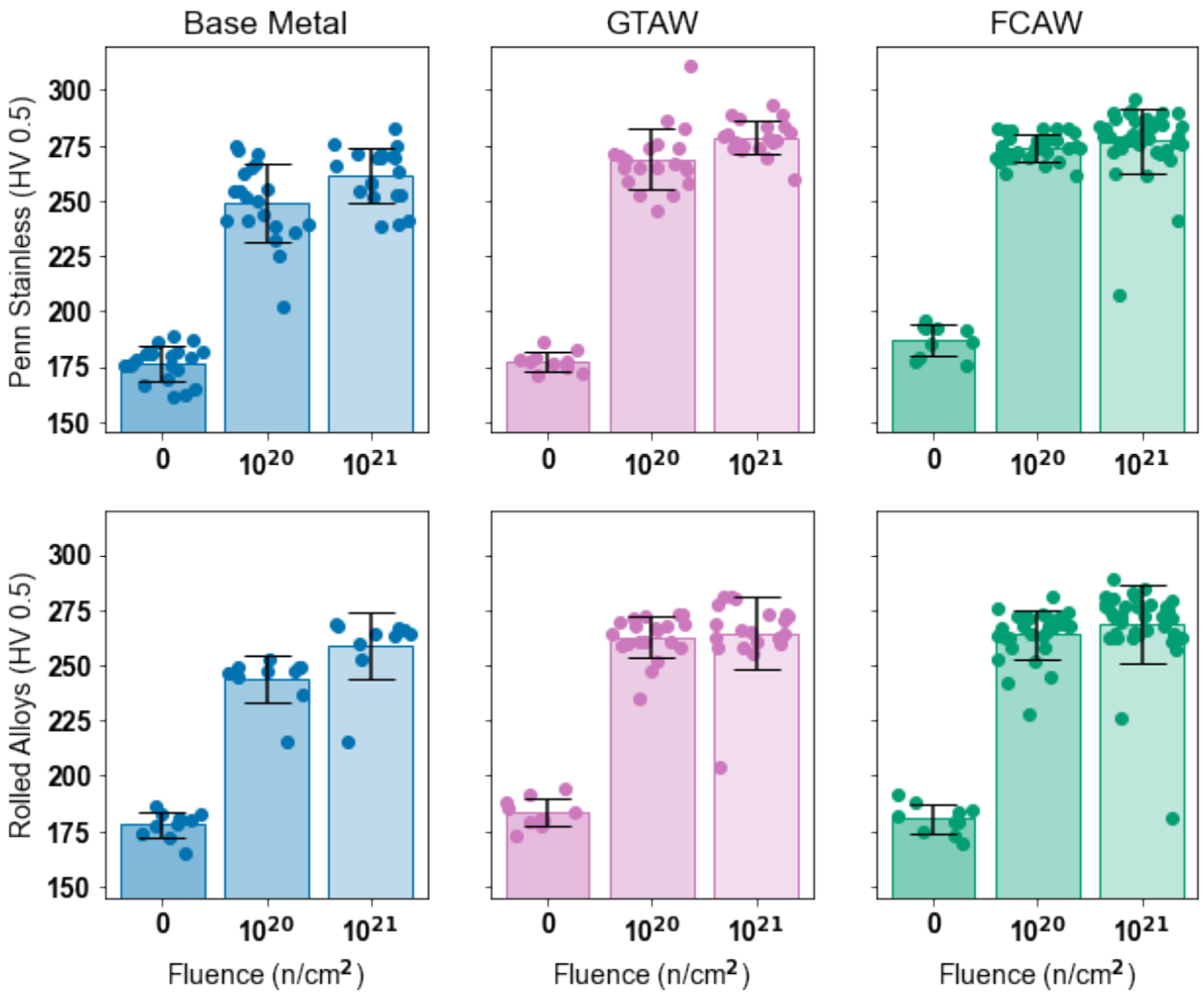

Figure 12. Microhardness of the AISI 347 produced by Penn Stainless and Rolled Alloys before and after irradiation and with or without a weld. These data points were all taken in the tab region of the specimens, so outside the fusion and heat affected zones of the welds. The error bars represent the standard deviation of the data points.

Select Rolled Alloys and Penn Stainless welded samples were hardness tested along the tensile axis to test the hardness across the base metal, heat affected zone, fusion zone, heat affected zone, and base metal. The Rolled Alloys unirradiated GTAW sample RTS35 is shown in Figure 13 as tested on the Wilson VH3100 microhardness tester with Buehler DiaMet software. The sample was cut so that the fusion zone center is at the center of the sample, so the color-coded indents show the hardness increases in the heat affected zones and fusion zone at the center of the sample. Comparing the Rolled Alloys unirradiated GTAW sample RTS35 and the FCAW sample RFS15 in Figure 14, there is not a significant difference in the hardness profile. The dotted lines on the graph show the average hardness in the tab region of each sample, which should correspond to the base metal value. There is a slight difference in these average values of hardness in the tabs, but only attributable to the spread of the data. The FCAW weld at the top is wider than the GTAW weld because of the shape of the bar (Figure 5) but both FCAW and GTAW weld bars have a different width with depth, so both samples were cut from a similar depth (layer 5 as in Figure 6b). Any difference in the width of the fusion zone is not observable in the microhardness line scans (Figure 14), but both the FCAW and GTAW samples show an increased microhardness in the heat affected zone and the fusion zone.

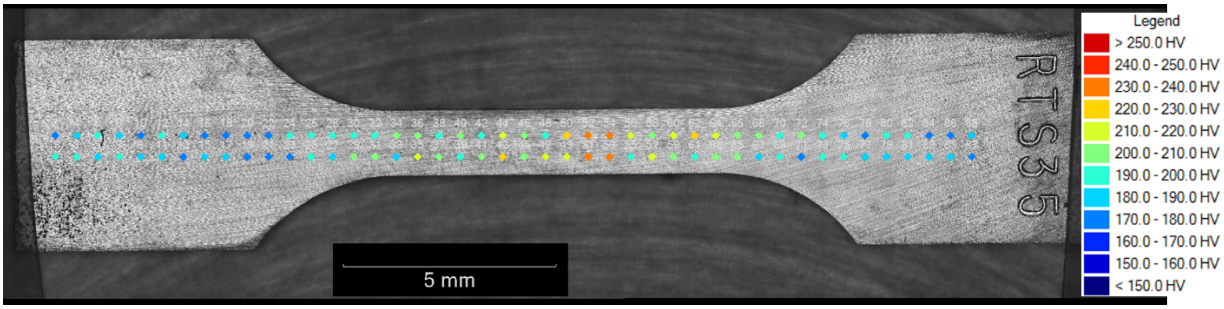

Figure 13. Optical image of sample RTS35 with two rows of hardness indents along the tensile axis. The indents are color-coded by hardness value.

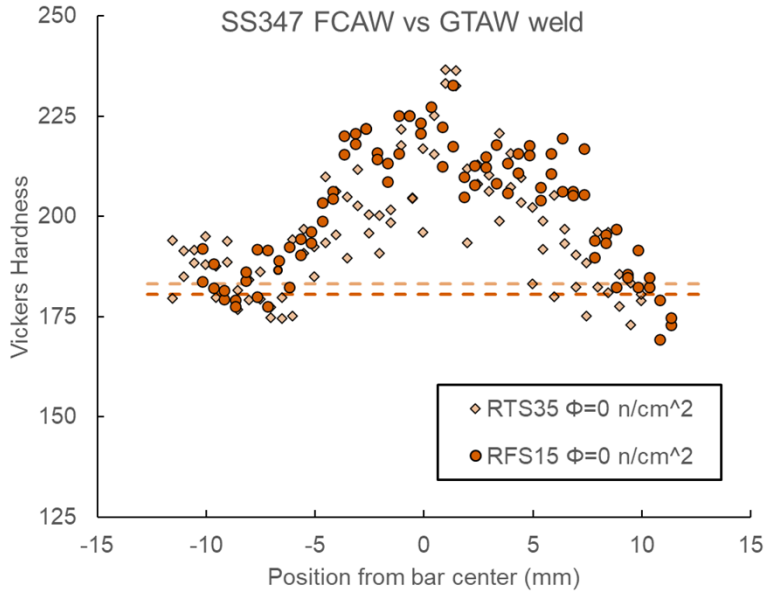

Figure 14. Comparison of the microhardness line scans from the Rolled Alloys unirradiated GTAW sample RTS35 and the FCAW sample RFS15. The dotted lines represent the average microhardness in the tab regions, representing the base metal value.

For the irradiated samples, there were only two samples of each type irradiated, and any sample that was hardness tested in the gauge section could not be tensile tested. Also, the unirradiated results of the line scan on the FCAW and GTAW samples were quite similar. Thus, only one of each of the higher irradiation dose FCAW weld samples were selected for the microhardness line scan and the other samples were tensile tested instead. The samples selected was the Rolled Alloys FCAW sample RFS35 and the Penn Stainless FCAW sample PFS35, both irradiated to 1.32E21 n/cm^2. Examining the Rolled Alloys unirradiated versus irradiated tests (Figure 15), the entire profile for the irradiated sample is higher than the unirradiated sample. The difference in hardness from the center of the fusion zone to the base metal in the tab regions is higher in the unirradiated sample than in the irradiated sample. The irradiated FCAW Penn Stainless and Rolled Alloys samples had very similar hardness profiles (Figure 16). This is as expected because the unirradiated base metal hardness is very similar for the two materials, and the same weld filler and weld procedure was used on both suppliers' materials.

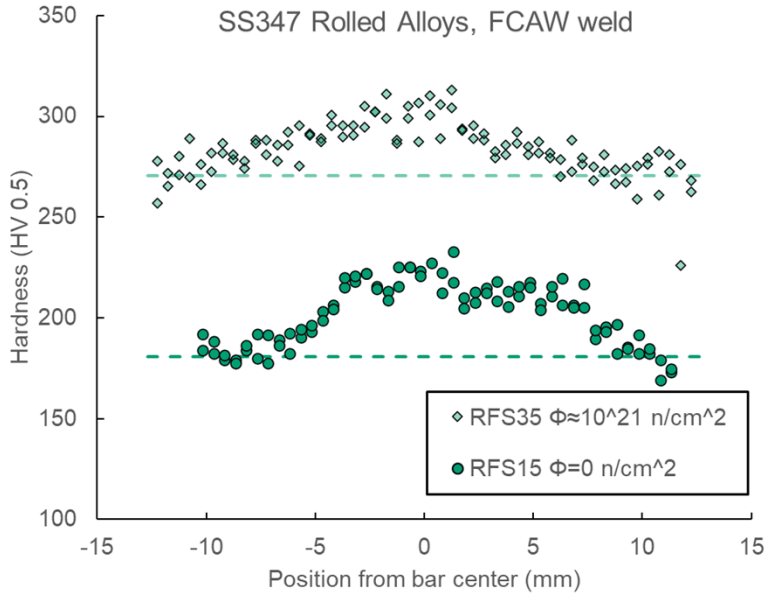

Figure 15. Microhardness indents along the tensile axis of the Rolled Alloys unirradiated and irradiated FCAW samples. The dotted lines indicate the average hardness in the tab regions of the samples, representing the base metal.

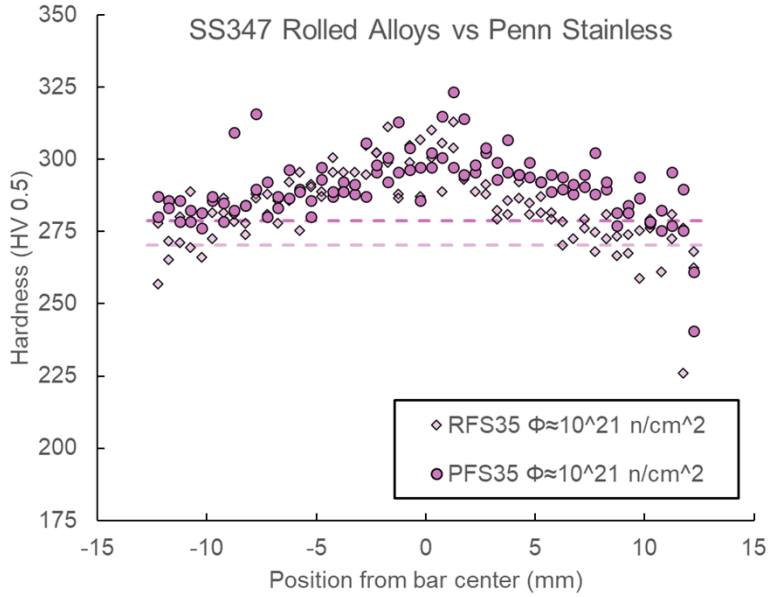

Figure 16. Comparison between the microhardness of the Rolled Alloys (RFS35) and Penn Stainless (PFS35) FCAW irradiated samples. The dotted lines indicate the average hardness in the tab regions of the samples, representing the base metal.

3.1.2 Tensile Properties

The base metal AISI 347 tensile properties from the first group of irradiations are repeated here for comparisons with the welded samples. For all three suppliers of base metal, the yield stress (YS) and

ultimate tensile strength (UTS) increased with increasing dose, while the uniform elongation (UE) and total elongation (TE) decreased Figure 17. The values of these properties were also very similar across the suppliers. For Sandmeyer Steel and Rolled Alloys, the A and B direction tensile properties were very similar, so only the A direction samples were irradiated. Penn Stainless had a more noticeable difference between A, the rolling direction, and B perpendicular to the rolling direction, so both were included in the group 1 irradiation capsules. The welded samples are in direction B, so the closest comparison is between the Penn Stainless B orientation base metal samples and the Penn Stainless FCAW and GTAW samples. For Rolled Alloys, the samples that were irradiated are the base metal in the A orientation and the FCAW and GTAW samples which correspond to the B orientation of the base metal. However, again, the A and B tensile properties of Rolled Alloys were not significantly different, so comparing the irradiated Rolled Alloys A orientation base metal to the Rolled Alloys irradiated FCAW and GTAW samples is reasonable.

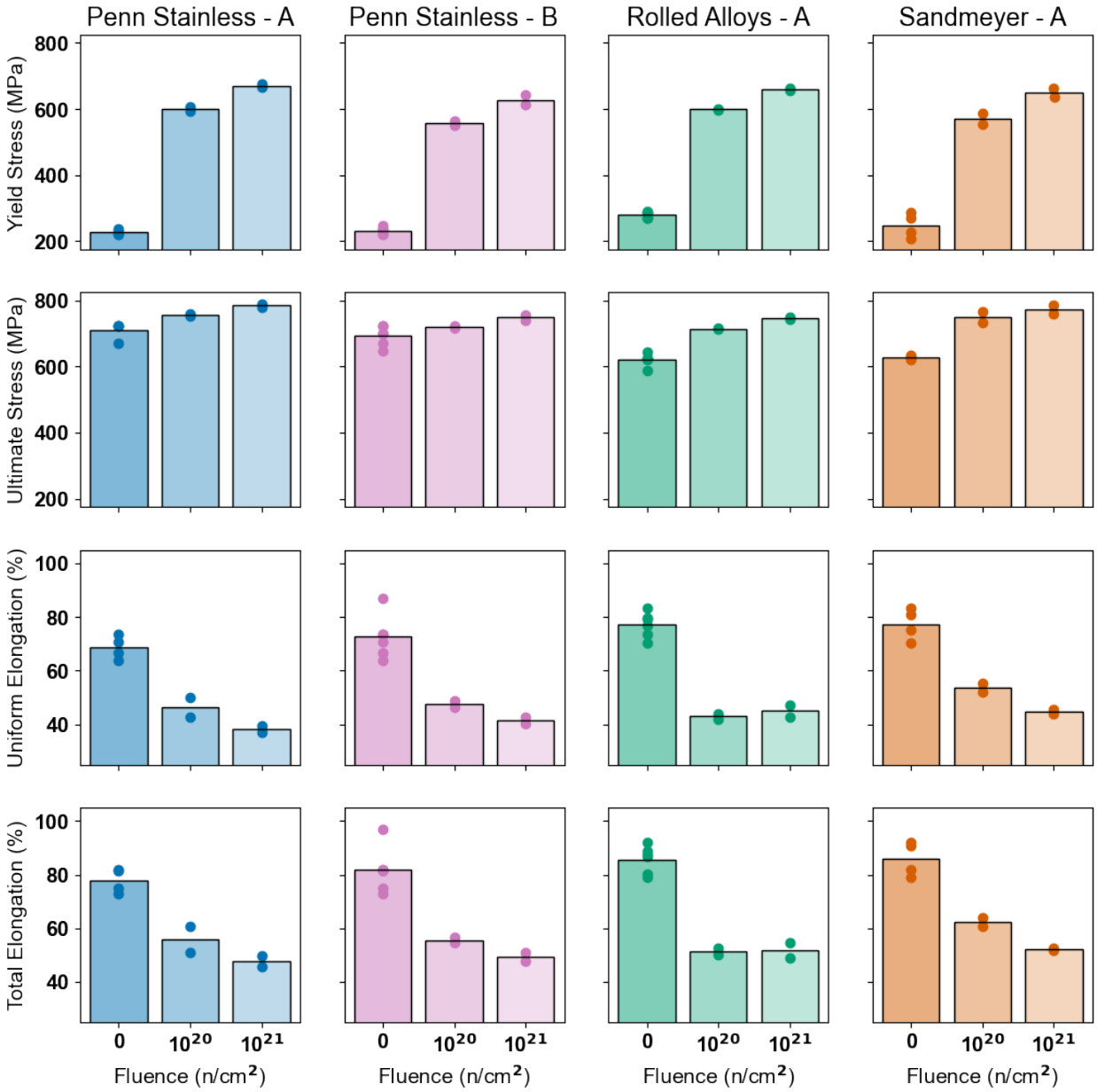

Figure 17. Summary of the tensile properties of the base metal AISI 347 steels (i.e., not welded samples). This is reprinted from [5].

The summary of welded tensile properties are shown in Figure 18. Both the Rolled Alloys and Penn Stainless FCAW samples had significantly lower TE than their base metal counterparts, with the FCAW samples irradiated to 10^{21} n/cm^2 had TE in the range of 20-35% while the base metal irradiated to the same condition had TE of 48-55%. GTAW samples had slightly higher TE than the FCAW type samples across the irradiation conditions.

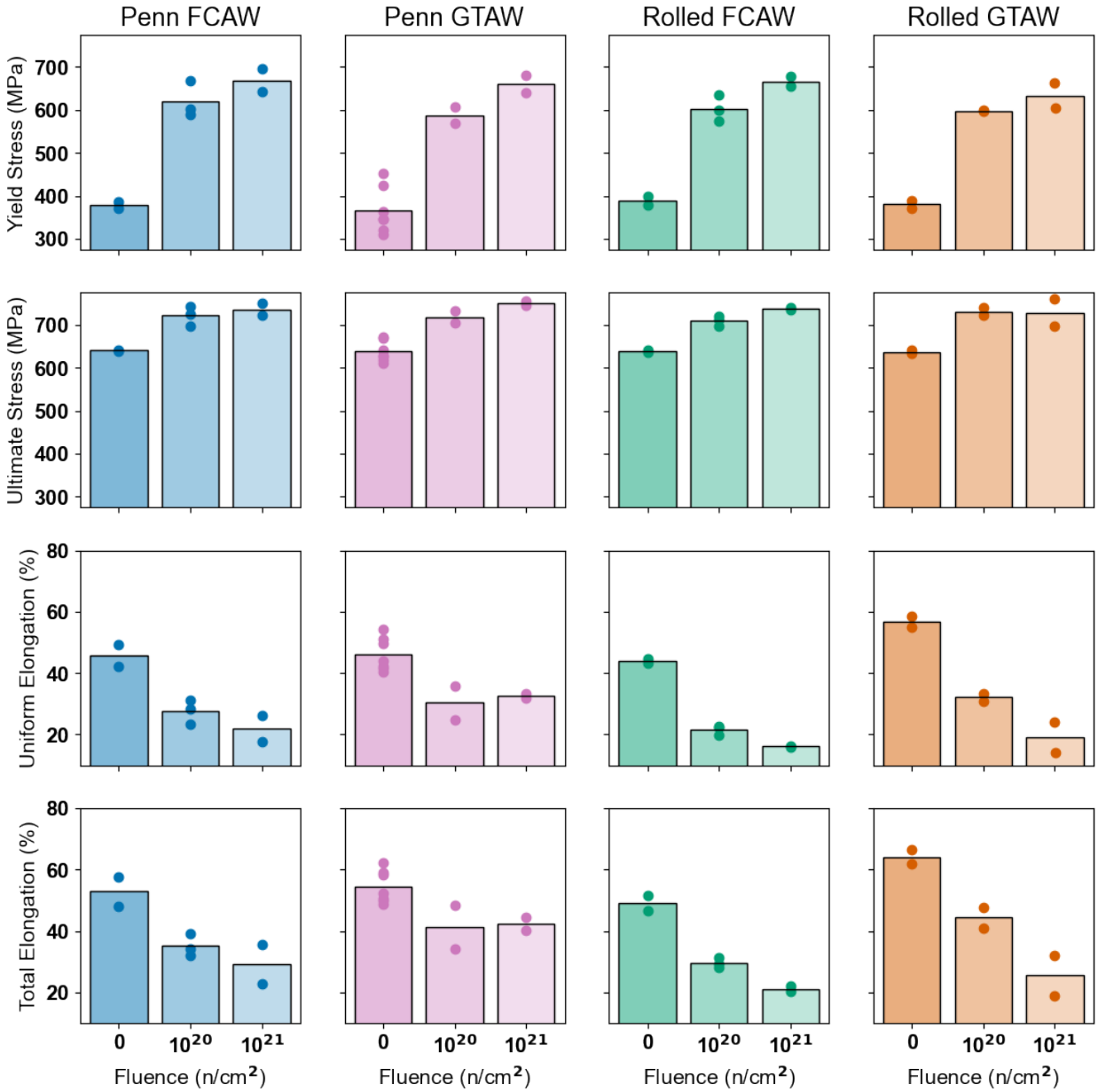

Figure 18. Summary of tensile properties of the welded samples of AISI 347.

More detail of the effects of irradiation can be seen in the tensile curves. Penn Stainless base metal is shown in Figure 19 as was reported in [5]. As the irradiation dose increased, the YS increased and the shape of the tensile curve changed. In some specimens and initial load drop after yielding is also seen, and this is a common occurrence for irradiated stainless steel 347, for example observed in Ref. [7]. Comparing the base metal in Figure 19 to the welded samples in Figure 20, the overall trend and change

in the shape of the tensile curve is the same, but the main difference is the reduced elongation of the welded samples.

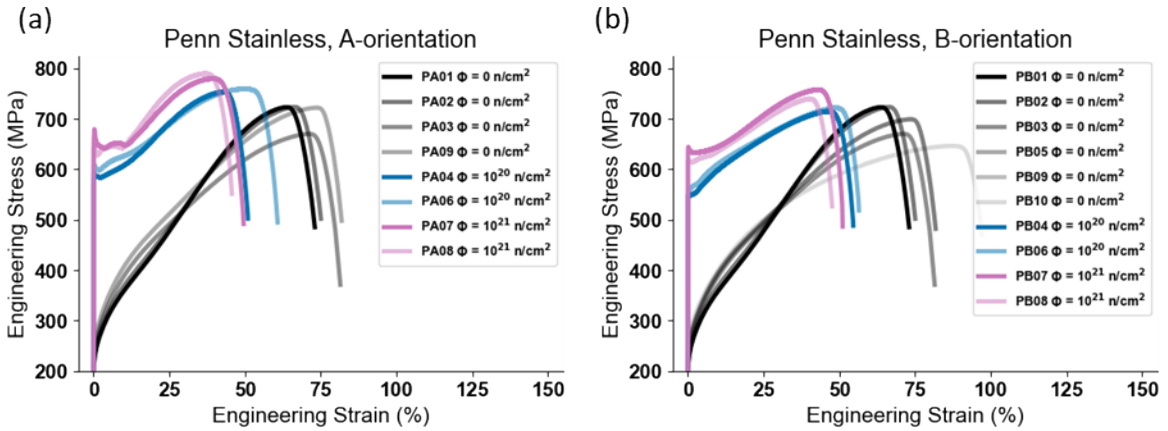

Figure 19. Penn Stainless base metal tensile curves. Reproduced from [5].

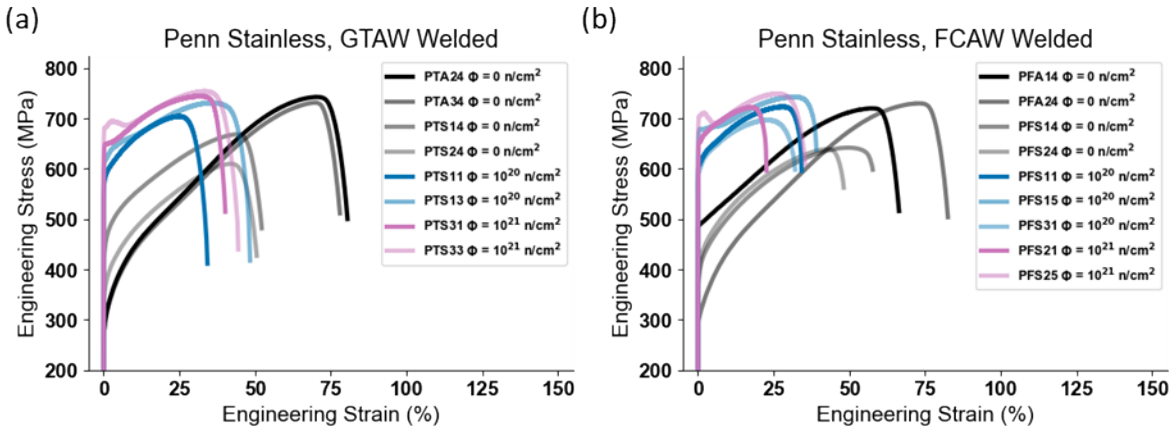

Figure 20. Penn Stainless tensile curves of the (a) GTAW and (b) FCAW samples.

As shown in Figure 5 and Figure 6, the weld bars had a V shaped joint, and the layer the sample was cut from was tracked during the machining. Samples with a lower sample number, such as PTS41, are from the top of the weld where the fusion zone is wider versus samples with a higher sample number, such as PTS45. There is a slight trend of decreased total elongation and increased ultimate tensile strength with increasing depth in the weld Figure 21.

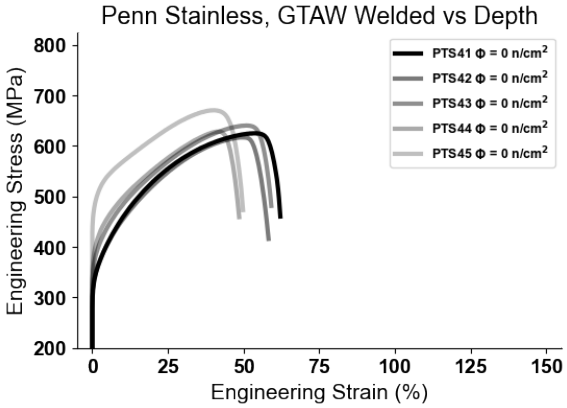

Figure 21. Tensile curves of Penn Stainless GTAW welded samples versus depth from the top of the weld. The lower the sample number, the wider the fusion zone of the weld is.

The Rolled Alloys and Sandmeyer Steel base metal tensile curves are shown in Figure 22 as was reported in [5]. Sandmeyer Steel was not selected for the welding trials, but is included here for comparison and completeness. The new data on the Rolled Alloys welded samples are shown in Figure 23. The Rolled Alloys and Sandmeyer base metal samples have a very similar shape in the unirradiated condition, but after irradiation, the load drop is more pronounced in the Sandmeyer samples. The Rolled Alloys GTAW and FCAW irradiated samples do not even show a load drop after the yield point Figure 23. As with the Penn Stainless welded and irradiated samples, there is a significant loss in elongation as compared to the base metal.

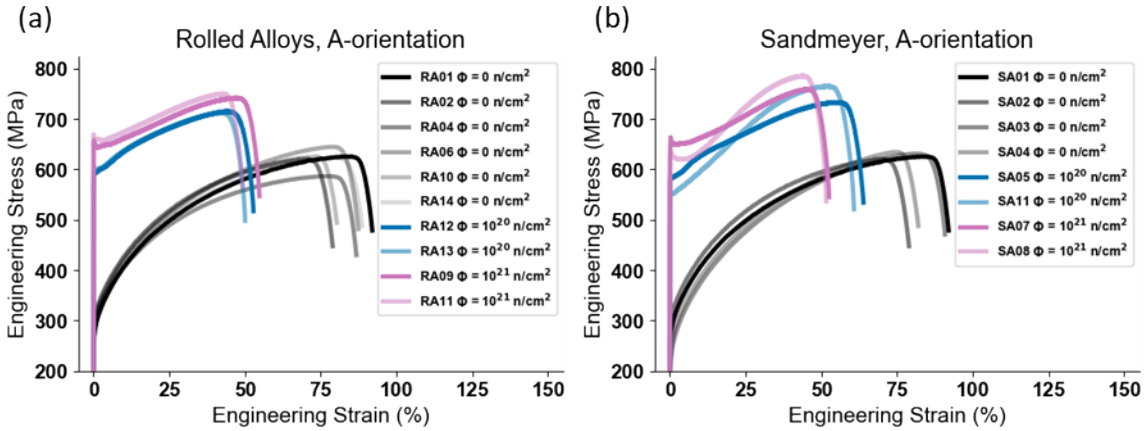

Figure 22. (a) Base metal Rolled Alloys tensile curves and (b) base metal Sandmeyer Steel tensile curves. Reproduced from [5].

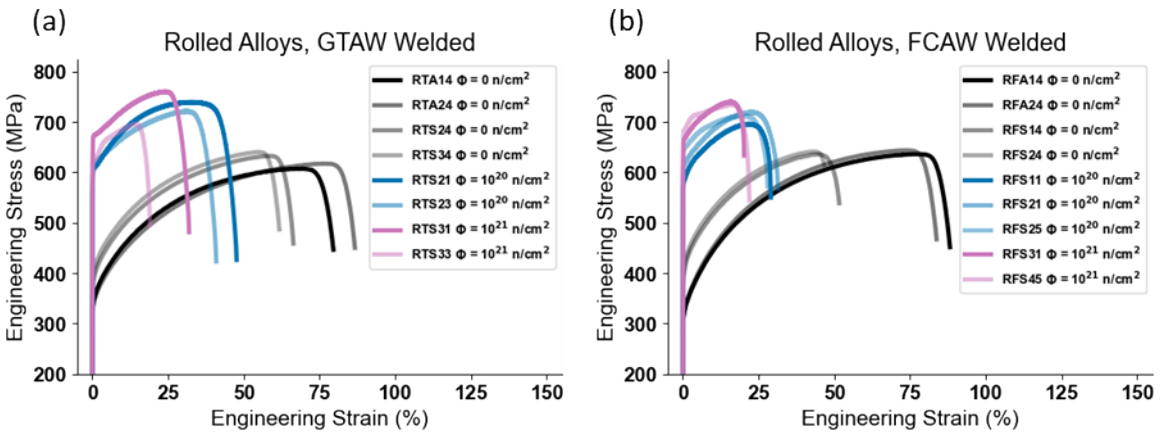

Figure 23. Tensile curves for the Rolled Alloys (a) GTAW and (b) FCAW welded samples.

3.2 EXPLOSION WELDED PLATE

3.2.1 Hardness Tests

The unirradiated explosion welded plate was polished in cross section and microhardness tested in a grid pattern to determine the hardness change across the interface Figure 24. Putting the pattern of indents on a diagonal relative to the interface allowed for more data points to be taken close to the interface. When these data points from the optical image in Figure 24 were plotted versus depth from the cladding surface in Figure 25, the trend can be easily seen. The hardness of the AISI 347 clad layer is overall harder than the alloy SA-516-70N base metal. However, because of the extreme plastic deformation that occurs during the bonding of the clad layer to the base plate, the clad layer's hardness sharply increases with depth from the surface and reaches a maximum at the interface. The alloy SA-516-70N base metal has a similar trend with a higher hardness immediately next to the interface and a lower hardness farther from the interface, but the magnitude of the difference is smaller than for the clad layer.

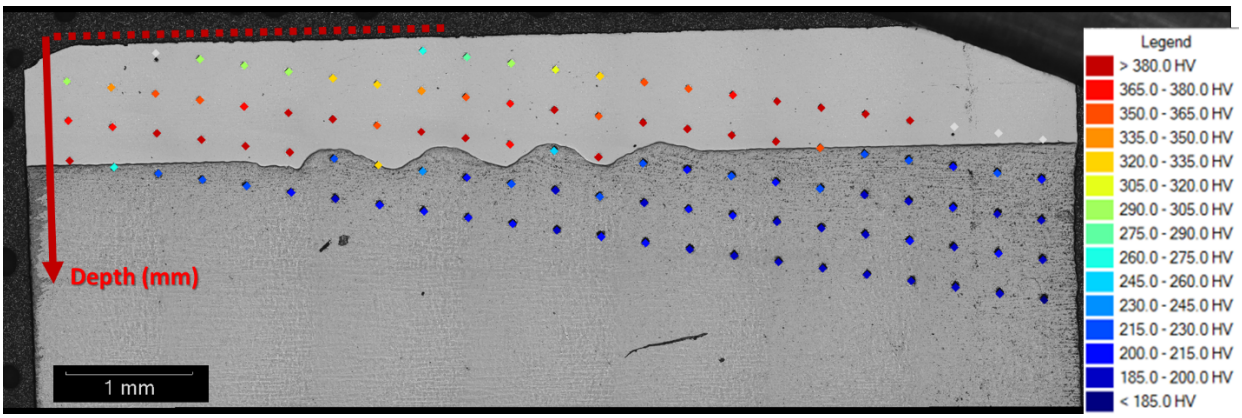

Figure 24. Optical image of cross section of unirradiated explosion welded plate with color coded microhardness indents.

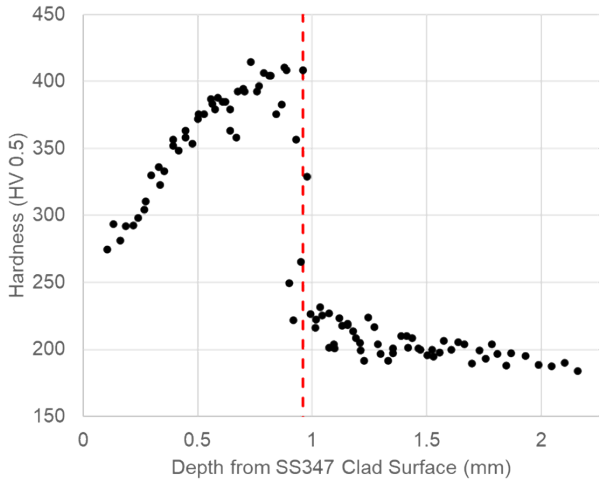

Figure 25. Plot of unirradiated microhardness versus depth from clad layer surface. The red dotted line denotes the interface between the cladding and the base metal.

The irradiated samples were cut so that one face of the tensile bar was entirely the clad layer and the other face was the base metal, as in Figure 7. The tensile samples were engraved with different characters on the clad and base metal side to track with material surface was being tested. For example, the sample listed as FC/FB-4 in Table 3 means the clad face was physically engraved with the characters "FC4" while the opposite side consisting of the base metal was engraved with the characters "FB4". In the Appendix Table 4, the hardness data is reported for each face separately using those labels. The data is plotted in Figure 26. The clad and base metal each have a large increase in hardness at 10^{20} n/cm^2 as compared to the unirradiated material, but there is only a slight difference between the material irradiated to the lower and higher neutron fluences. The AISI 347 clad layer remains significantly harder than the alloy SA-516-70N after irradiation.

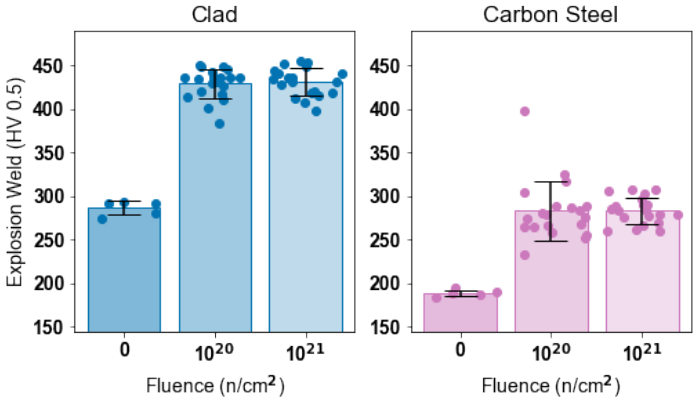

Figure 26. Vickers microhardness of the AISI 347 clad layer and the alloy SA-516-70N base metal side of the half and half samples.

3.2.2 Tensile Properties

The samples of the clad plate included in the irradiation group 2 capsules were half clad and half base metal as illustrated in Figure 7. Their tensile properties are summarized in Figure 27, with the detailed tensile curves in Figure 28 and the values in the Appendix Table 5. The alloy SA-516-70N base metal and the clad-only samples were not irradiated, so only their unirradiated properties are available. The base

metal has significantly lower YS and UTS than the clad-only samples, but the half and half type samples have a further increased strength. The half and half samples did not have a dramatic increase in strength after irradiation. The UE is similar for the base metal and clad before irradiation and reduces slightly after irradiation. The TE has a more significant effect, where the base metal and clad-only samples have similar elongations of 12-13%, but the half and half samples unirradiated only have about 9% TE, and there is a sharp drop in elongation for the irradiated half and half samples to 0.8-1.6%. The shape of the tensile curves do not change after irradiation (Figure 28) as was seen in the AISI 347 irradiated materials (Figure 19 and Figure 22).

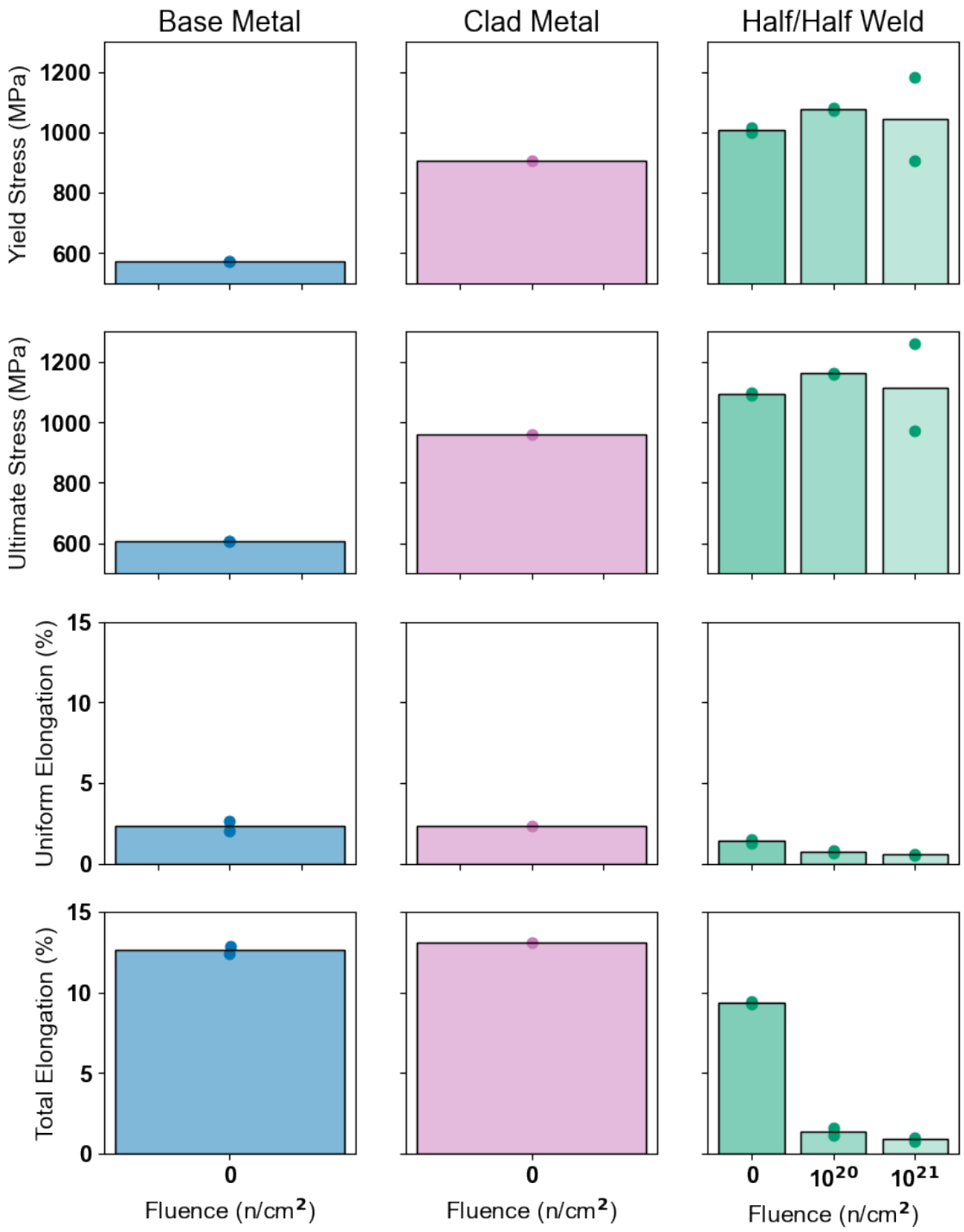

Figure 27. Summary of the tensile properties of the explosion welded samples.

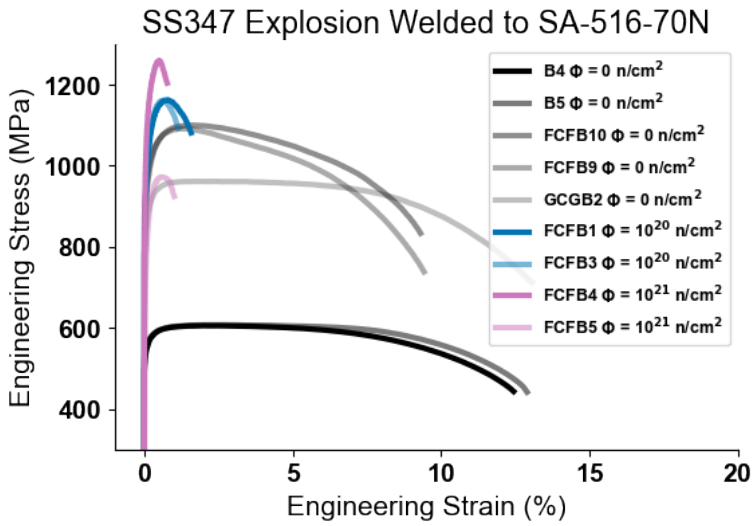

Figure 28. Tensile curves of the explosion welded material before and after irradiation. Samples labeled B are base metal, GCGB is clad only, and FCFB are half clad and half base metal.

3.3 ZIRCALOY-4

3.3.1 Hardness Tests

For the Zircaloy-4 samples in the second group of irradiations, it was decided to prioritize tensile tests over the microhardness line scans, so only microhardness indents in the tab regions were performed. This is supported by the results from the first group of irradiation capsules in which the line scan hardness tests on the welded Zircaloy-4 samples did not show a significant difference between the base metal, heat affected zone, and fusion zone [5]. The details of the microhardness values are in the Appendix Table 4. One example of the indent pattern on an unirradiated Zircaloy-4 tensile tab is shown in Figure 29. This is the same way that the tab indents were performed on the AISI 347 samples as well.

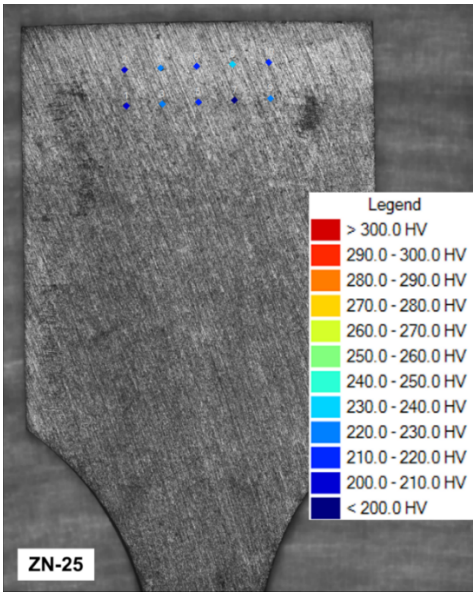

Figure 29. Optical image of sample ZN-25 showing the ten hardness indents in the tab region of the tensile sample.

The irradiated Zircaloy-4 materials compared several conditions including irradiation dose, PWHT, and H content. The details of the conditions including the H charging amount in ppm are listed in Table 3. The H charged samples were divided into low or high levels of H content, which were roughly 200 or 400 ppm respectively. When Zircaloy-4 is used in an aqueous environment, it has the potential to absorb H, which will precipitate into a brittle zirconium hydride phase. At room temperature the terminal solid solubility of H in Zircaloy is less than 1 ppm [8], so all H charged samples tested here will have precipitated hydride phases. The hydride platelets nucleate and grow from the grain boundaries [9]. In a water and irradiation environment such as the SHINE system, the main sources of H are from aqueous corrosion of the Zircaloy-4 or the radiolytic decomposition of water [8]. The microhardness for all the irradiated samples was taken near the edge of the tab section as in Figure 29.

For essentially all conditions the microhardness increased with increasing neutron dose Figure 30. For those cases where the average microhardness did not increase with increasing dose, there was also a large scatter in the data points. The microhardness also generally increased with increasing H content. For any H content, the difference in microhardness between the PWHT and non PWHT samples was minor.

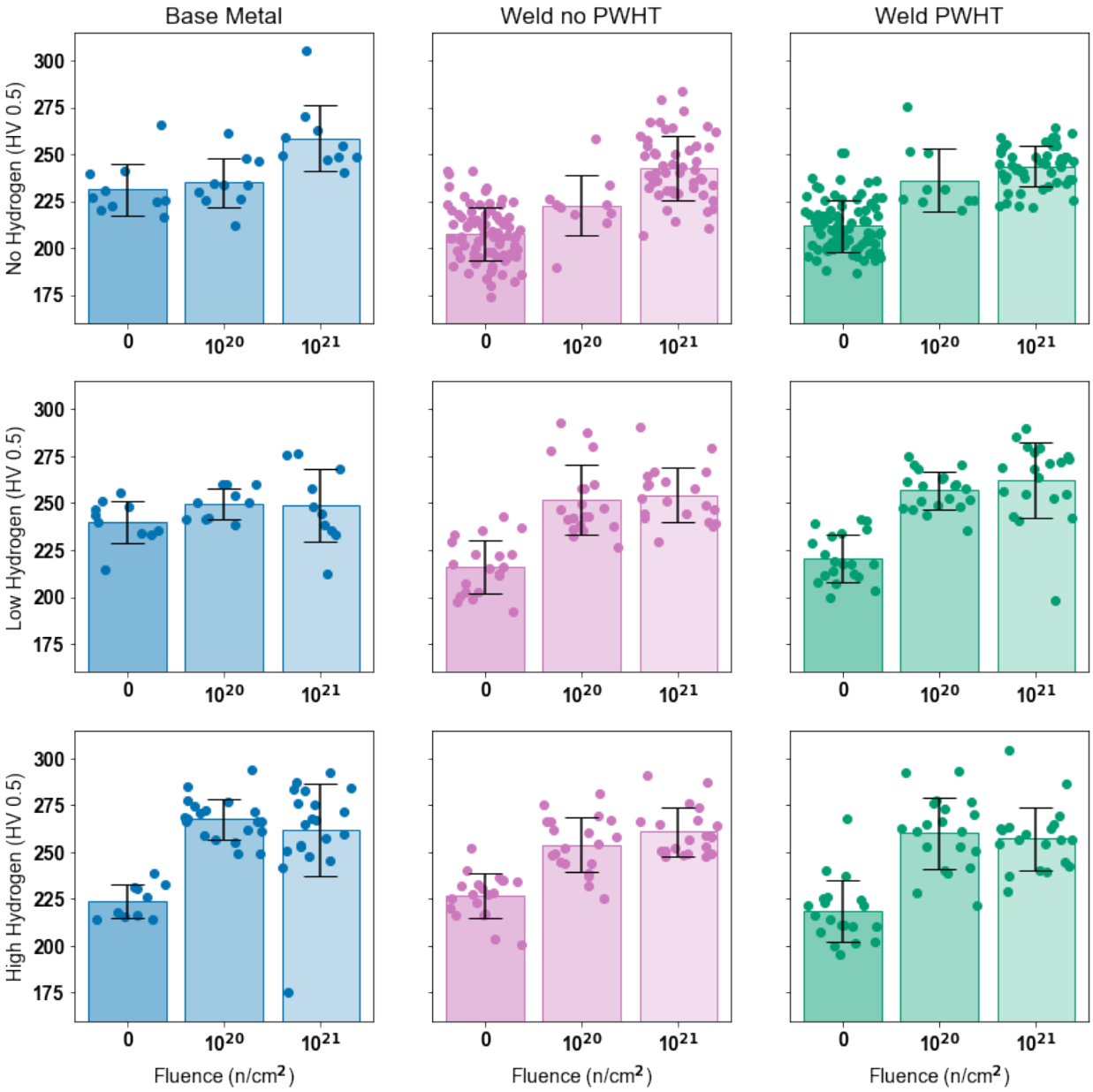

Figure 30. Microhardness of Zircaloy-4 samples, comparing irradiation dose, hydrogen content, and weld PWHT.

3.3.2 Tensile Properties

The summary of Zircaloy-4 base metal with varying levels of H charging are shown in Figure 31 with the values tabulated in the Appendix Table 5. With increasing H content, the YS and UTS slightly increased, and further increased with increasing neutron dose. Matching this, with increasing H content, the UE and TE decreased and further decreased with increasing neutron dose. The base metal without H (Figure 32) and the base metal with approximately 225 ppm H (Figure 33) were previously published with the group 1 irradiation capsule results [5] and are included here for comparison with the approximately 450 ppm H charged materials (Figure 34). The H charging does not change the shape of the curves, but it makes the samples more likely to prematurely break. Especially in the 450 ppm case this is seen for several of the unirradiated samples, that they start to follow the normal shape of the tensile curve but then end abruptly.

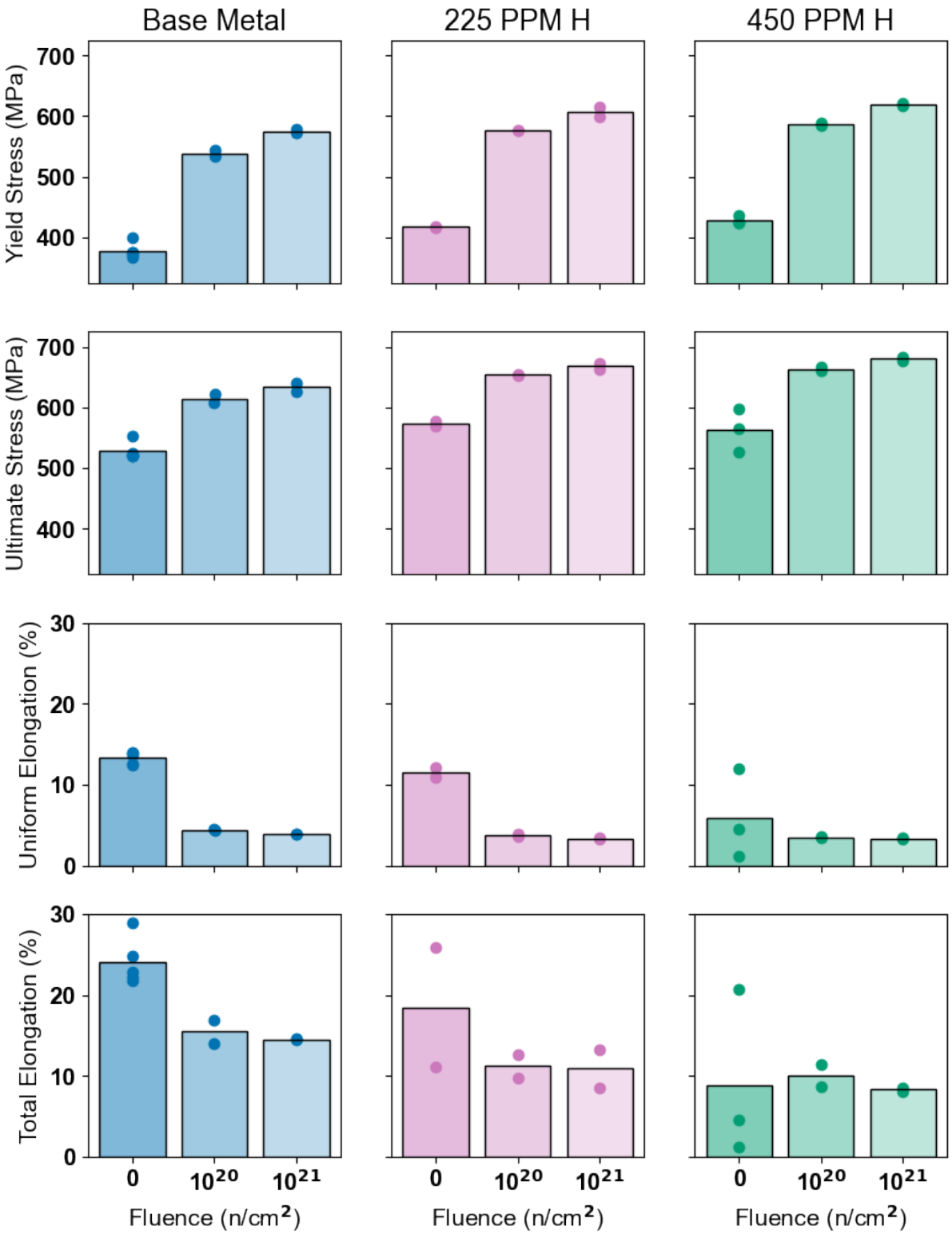

Figure 31. Tensile properties of the Zircaloy-4 base metal with varying levels of H charging.

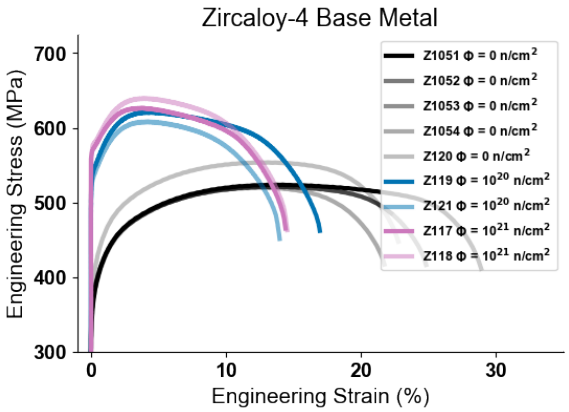

Figure 32. Zircaloy-4 base metal tensile curves. Reproduced from [5].

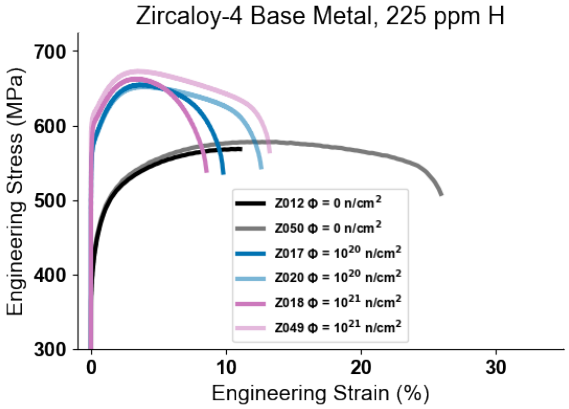

Figure 33. Tensile curves of the Zircaloy-4 base metal with approximately 225 ppm H. This figure is reproduced from [5].

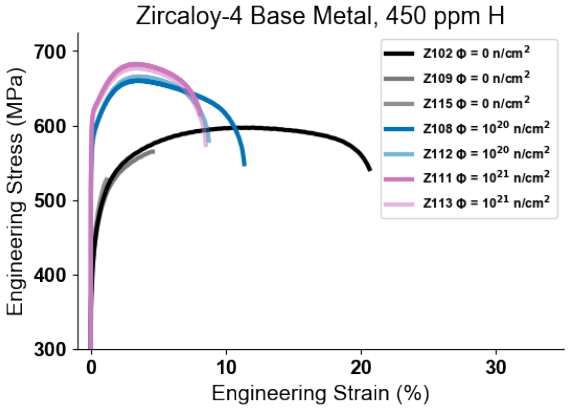

Figure 34. Zircaloy-4 base metal charged with approximately 450 ppm H and tensile tested.

Next, the Zircaloy-4 welded samples without a PWHT and with varying amounts of H are summarized in Figure 35. This represents the worst case scenario for the Zircaloy-4 because the PWHT is designed to recover some of the ductility of the welded material and the H charging makes the samples more brittle as well.

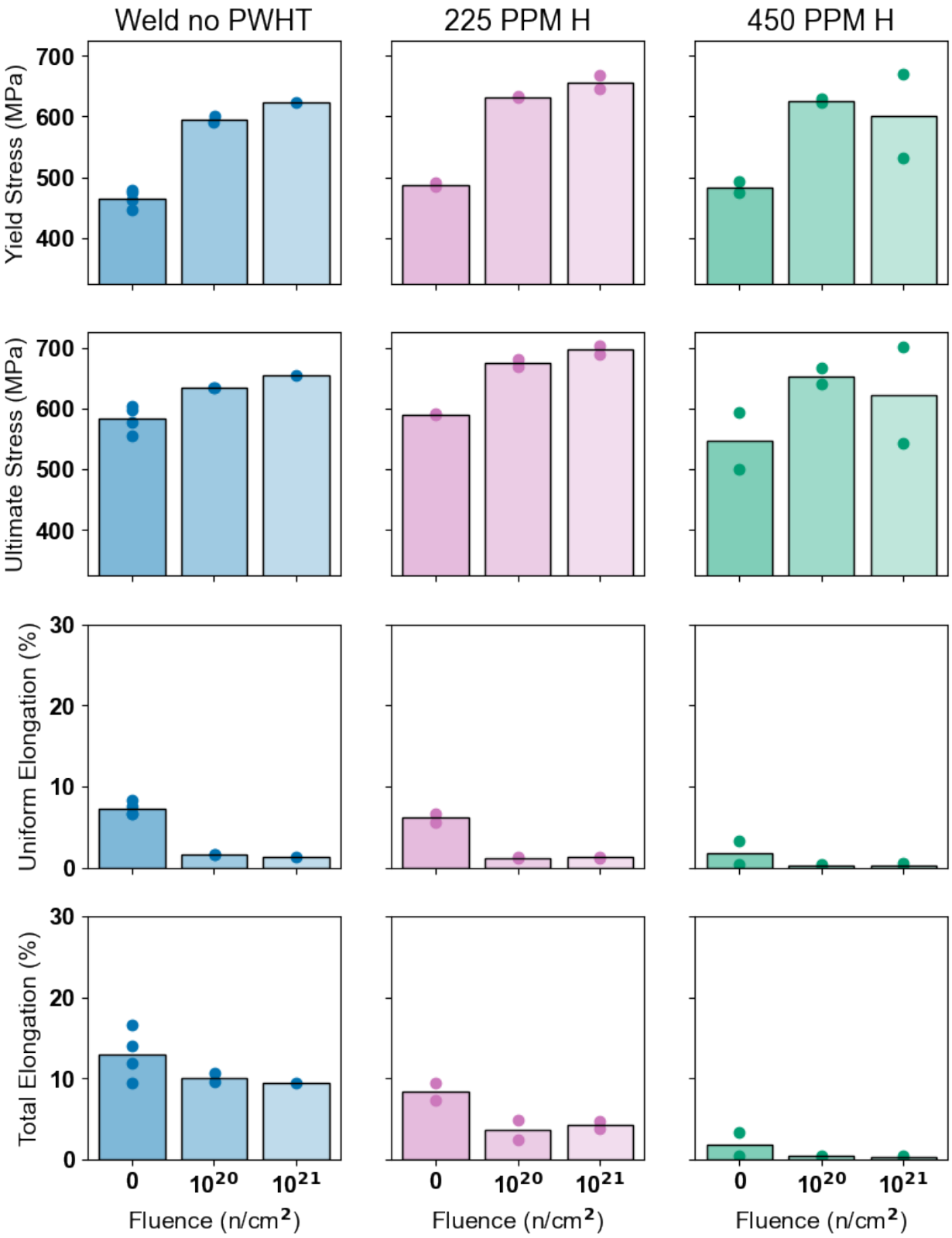

Figure 35. Tensile property summary for the Zircaloy-4 welded samples without a PWHT and with varying levels of H. The no H column of data was replotted from [5].

The previously reported tensile results for the Zircaloy-4 welded but without a PWHT are shown in Figure 36. The welding significantly reduces the elongation as compared to the base metal (Figure 32). With increasing amounts of H charging, the elongation is further reduced (Figure 37 and Figure 38). The samples without the PWHT and with ~450 ppm H have the worst elongation of any of the Zircaloy-4 conditions tested.

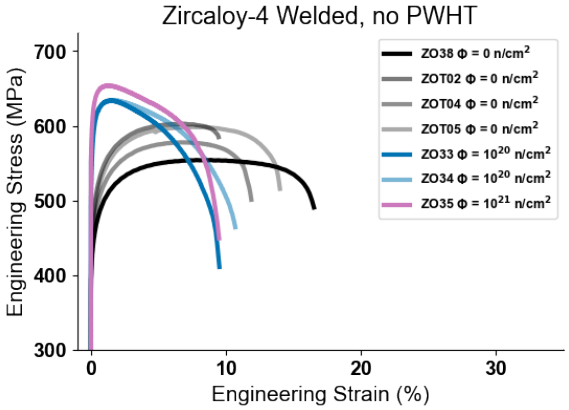

Figure 36. Tensile curves for welded Zircaloy-4 without a PWHT and without any H charging. Reprinted from [5].

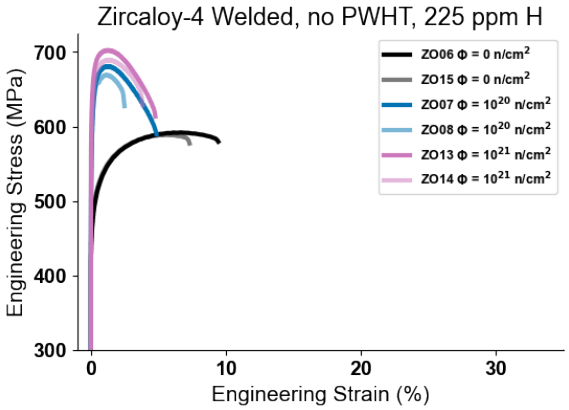

Figure 37. Zircaloy-4 welded samples without a PWHT and with approximately 225 ppm H.

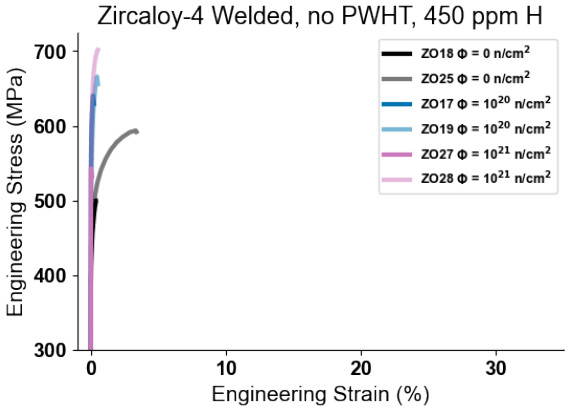

Figure 38. Tensile curves for Zircaloy-4 welded samples without a PWHT and with approximately 450 ppm H.

A slight improvement on the as-welded samples is seen in those that had a PWHT for 1 h at 600°C, summarized in Figure 39 and with the values tabulated in Appendix Table 5. The order of sample preparation was welding, PWHT, sample cutting, and finally the H charging. Thus the PWHT had no effect on the H content or structure; it only recovered some of the microstructure in the welded bar before the H was introduced. The welded and PWHT material (Figure 40) recovered a slight amount of ductility as compared to the no PWHT materials (Figure 36). With the addition of H, the welded and PWHT samples still have a reduction in ductility (Figure 41 and Figure 42) but it is not as severe as the no PWHT samples. Especially at the highest level of H charging, the no PWHT samples have mostly brittle failure (Figure 38) while those with the same level of H charging but with a PWHT show a small amount of ductility (Figure 42). This potential for severely reduced ductility or even brittle failure when Zircaloy-4 is exposed to H and neutron irradiation is one of the main reasons the SHINE program shifted to focus on the AISI 347 which does not have a similar concern.

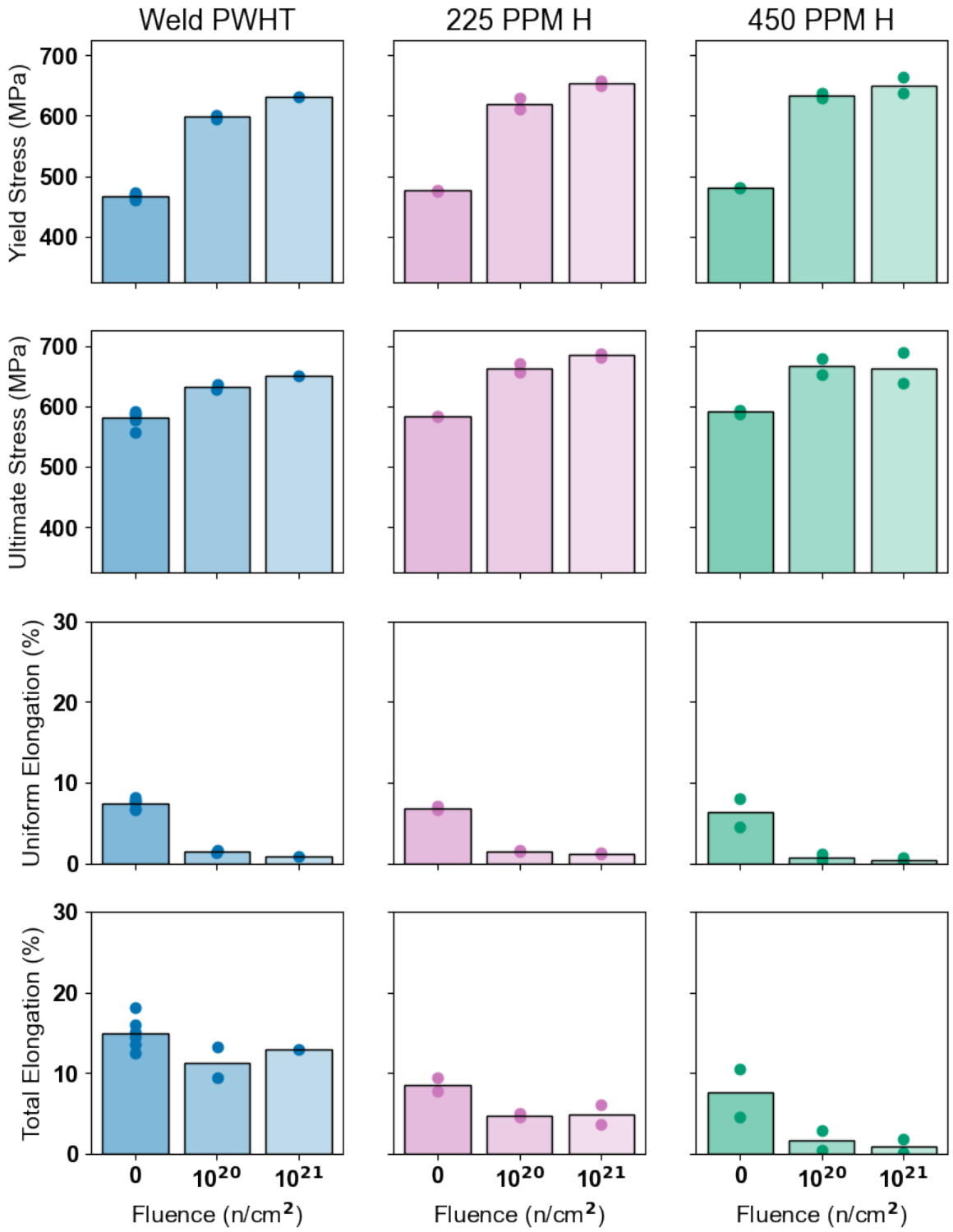

Figure 39. Tensile property summary for the Zircaloy-4 welded samples that had a 1 h at 600°C PWHT and with varying levels of H charging. The column of data without H charging is reprinted from [5], while the H containing samples are new data reported here.

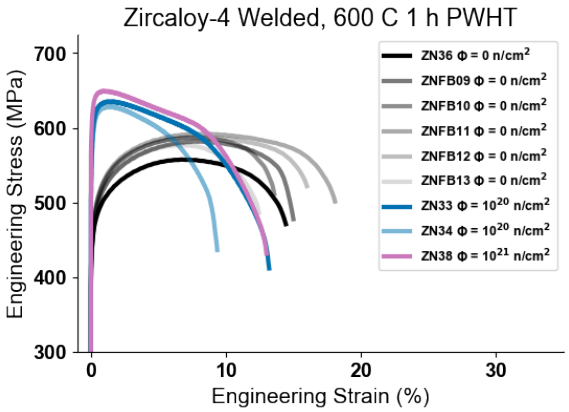

Figure 40. Zircaloy-4 welded and PWHT tensile curves. This is reprinted from [5].

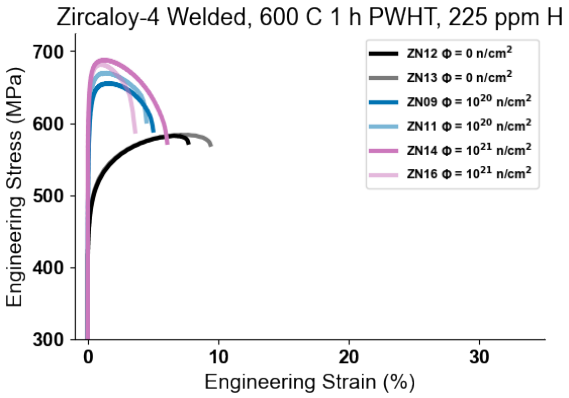

Figure 41. Tensile curves for Zircaloy-4 welded and PWHT with approximately 225 ppm H.

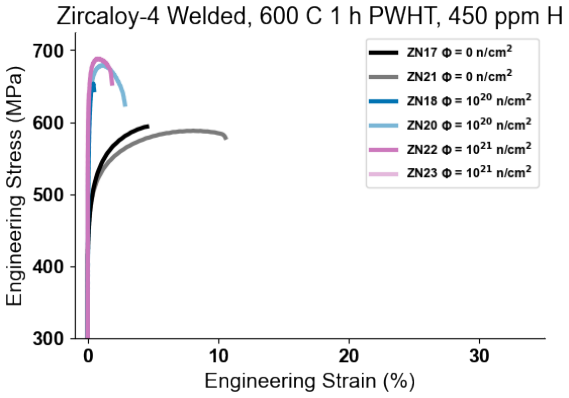

Figure 42. Tensile curves for Zircaloy-4 welded and PWHT with approximately 450 ppm H.

4. SUMMARY

This report concludes the series of reports investigating Zircaloy-4 and AISI 347 for the SHINE medical isotope facility. Here, the second group of irradiation capsule microhardness and tensile results were presented and compared to the results from the first group of irradiation capsules. The second group of samples included the welded AISI 347, explosion welded AISI 347 clad to alloy SA-516-70N base metal, and welded and H charged Zircaloy-4. The welded AISI 347 of all types had an increased hardness in the fusion zone, whereas the previously irradiated welded Zircaloy-4 samples showed more uniform hardness across the fusion zone. All samples experienced increased strength and decreased ductility with increasing neutron dose. The Zircaloy-4 welded samples had a more severe loss in ductility with TE <10%, while the AISI 347 welded and irradiated samples maintained >20% TE even at the highest dose. Additionally, of all samples tested, the Zircaloy-4 welded without a PWHT and with H charging had the worst performance with entirely brittle fractures. For the SHINE facility that will experience neutron irradiation and water exposure at low temperatures (<100°C), AISI 347 appears to be the better choice of material.

5. REFERENCES

[1] C. Silva, C. Bryan, Evaluation of Zircaloy-4 as the structural material for the Target Solution Vessel and support lines of SHINE — Sample preparation for the third-round neutron irradiation, Oak Ridge National Laboratory, FY17 Report, ORNL/TM-2017/482, (2017)
[2] L. Garrison, C. Silva, B. Eckhart, C. Bryan, Evaluation of Zircaloy-4 Welding and Hydrogen Charging Effects for Use as the Structural Material for the Target Solution Vessel and Support Lines of SHINE, Oak Ridge National Laboratory, ORNL/TM-2018/1035, (2018)
[3] L.M. Garrison, J.R. Echols, K. Bawane, B. Eckhart, C. Bryan, Zircaloy-4 and Stainless Steel 347 Property Data and Microstructures Related to the Structural Material for the Target Solution Vessel and Support Lines of SHINE, Oak Ridge National Laboratory, ORNL/SPR-2019/1356, (2019) 1-38.
[4] L.M. Garrison, J. Echols, N. Reid, C. Bryan, Welded and Hydrogen Charged Zircaloy-4 and Welded Stainless Steel 347 Property Data and Microstructures for the Target Solution Vessel and Support Lines of SHINE, Oak Ridge National Laboratory, ORNL/SPR-2020/1879, (2021) 1-56.
[5] J. Echols, N. Reid, J. Reed, X. Chen, C. Bryan, L.M. Garrison, Property data of irradiated SS 347 and irradiated, welded, and hydrogen charged Zircaloy-4 for the target solution vessel and support lines of SHINE, Oak Ridge National Laboratory, ORNL/SPR-2021/2397, (2022) 1-29.
[6] L.M. Garrison, Y. Katoh, N.A.P. Kiran Kumar, Mechanical properties of single-crystal tungsten irradiated in a mixed spectrum fission reactor, Journal of Nuclear Materials 518 (2019) 208-225.
[7] H.R. Higgy, F.H. Hammad, Effect of fast-neutron irradiation on mechanical properties of stainless steels: AISI types 304, 316, and 347, Journal of Nuclear Materials 177-186 (1975) 177-186.
[8] S. Suman, M.K. Khan, M. Pathak, R.N. Singh, J.K. Chakravartty, Hydrogen in Zircaloy: Mechanism and its impacts, International Journal of Hydrogen Energy 40(17) (2015) 5976-5994.
[9] G. Bertolino, G. Meyer, J. Perez Ipina, Degradation of the mechanical properties of Zircaloy-4 due to hydrogen embrittlement, Journal of Alloys and Compounds 330-332 (2002) 408-413.

6. APPENDIX

Table 4. The average and standard deviation for all irradiated samples that were microhardness tested. A minimum of 20 data points were taken from each sample, 10 from each tab of the tensile bar. The B or T at the end of a sample ID means the top or bottom row of indents for samples where two lines of hardness indents were performed along the tensile axis.

Sample ID	Average Hardness (HV)	Standard Deviation (HV)
FB1	267	16.0
FB3	300	38.4
FB4	288	16.7
FB5	280	12.0
FC1	435	16.7
FC3	425	15.6
FC4	424	12.0
FC5	439	16.0
PA02	174	8.6
PA06	258	20.1
PA07	265	9.5
PB02	179	5.6
PB04	240	7.5
PB07	257	13.8
PFS11	274	6.2
PFS15	271	5.7
PFS21	284	6.0
PFS25	267	20.9
PFS35B	278	13.6
PFS35T	280	7.4
PFS41	276	5.3
PFS45	187	7.0
PTS11	269	9.6
PTS13	269	16.8
PTS31	280	7.5
PTS33	277	7.2
PTS35	177	4.4
RA02	178	5.7
RA09	259	15.2
RA13	244	10.3
RFS11	264	14.0
RFS15	181	6.6
RFS21	262	10.6

RFS25	265	6.2
RFS31	263	27.9
RFS35B	272	10.1
RFS35T	269	15.0
RFS45	271	7.1
RTS21	266	6.4
RTS23	259	10.6
RTS31	272	7.9
RTS33	257	18.3
RTS35	183	6.2
SA02	187	5.3
SA07	261	8.3
SA11	234	8.1
Z107	224	8.7
Z108	271	12.0
Z111	270	14.8
Z112	264	8.4
Z113	254	29.6
Z117	259	17.5
Z119	235	13.0
Z12	240	11.2
Z120	231	13.7
Z17	250	8.3
Z18	249	19.4
ZN02	224	12.1
ZN09	256	9.6
ZN11	258	10.3
ZN12	218	12.5
ZN14	263	14.8
ZN16	262	24.5
ZN18	261	24.0
ZN20	259	12.0
ZN21	221	19.7
ZN22	256	15.7
ZN23	259	17.5
ZN25	216	11.1
ZN33	236	16.6
ZN35	212	13.6
ZN37	245	12.8
ZO02	226	11.8
ZO06	206	9.1

ZO07	256	22.6
ZO08	247	12.0
ZO13	251	15.8
ZO14	257	12.5
ZO17	252	13.5
ZO18	231	11.8
ZO19	255	15.3
ZO25	222	9.8
ZO27	265	14.7
ZO28	257	8.6
ZO34	223	16.1
ZO36	243	16.6
ZO37	208	14.2
EXWC	287	7.5
EXWB	189	3.7

Table 5. Tensile properties of the materials in this project, including unirradiated and irradiated in group 1 and 2.

Sample ID	Dose (n/cm^2)	Yield Stress (MPa)	Ultimate Tensile Stress (MPa)	Uniform Elongation (%)	Total Elongation (%)
B4	0	574	605	2.0	12.4
B5	0	575	608	2.7	12.9
FCFB1	1E+20	1073	1162	0.8	1.6
FCFB10	0	998	1100	1.5	9.3
FCFB3	1E+20	1080	1161	0.6	1.1
FCFB4	1E+21	1183	1259	0.5	0.8
FCFB5	1E+21	906	972	0.6	1.0
FCFB9	0	1015	1091	1.3	9.4
GCGB2	0	906	961	2.3	13.1
PA01	0	220	723	64.0	73.0
PA02	0	220	724	66.5	75.1
PA03	0	231	670	70.8	81.5
PA04	1E+20	593	754	42.7	51.0
PA06	1E+20	607	760	50.0	60.8
PA07	1E+21	677	780	39.3	49.6
PA08	1E+21	665	790	37.0	45.7
PA09	0	238	722	73.6	81.9
PB01	0	220	723	64.0	73.0
PB02	0	220	724	66.5	75.1
PB03	0	231	670	70.8	81.5
PB04	1E+20	549	715	46.4	54.6
PB05	0	237	699	73.5	81.8

PB06	1E+20	565	722	49.0	56.5
PB07	1E+21	643	758	42.8	51.1
PB08	1E+21	614	740	40.2	47.6
PB09	0	237	699	73.5	81.8
PB10	0	246	646	87.1	97.0
PFA14	0	486	720	57.4	66.4
PFA24	0	297	730	73.1	82.5
PFS11	1E+20	603	724	28.2	34.2
PFS14	0	372	642	49.1	57.7
PFS15	1E+20	667	744	31.3	39.1
PFS21	1E+21	642	723	17.6	22.7
PFS24	0	385	639	42.2	48.1
PFS25	1E+21	697	750	26.3	35.4
PFS31	1E+20	589	698	23.3	32.1
PTA24	0	284	743	69.8	80.5
PTA34	0	277	732	70.0	78.0
PTS11	1E+20	569	705	24.9	34.3
PTS13	1E+20	607	732	35.7	48.3
PTS14	0	425	669	44.0	52.2
PTS24	0	345	610	42.2	50.5
PTS31	1E+21	640	745	31.8	40.2
PTS33	1E+21	680	755	33.3	44.4
PTS41	0	311	625	54.3	62.1
PTS42	0	319	617	49.5	58.2
PTS43	0	347	641	51.0	59.2
PTS44	0	365	629	41.5	48.5
PTS45	0	453	671	40.3	49.8
RA01	0	269	626	83.3	92.0
RA02	0	287	621	70.5	78.9
RA04	0	288	587	76.9	86.8
RA06	0	271	645	79.2	87.4
RA09	1E+21	656	742	47.3	54.7
RA10	0	290	626	73.7	80.3
RA11	1E+21	664	750	42.8	49.1
RA12	1E+20	597	715	44.1	52.8
RA13	1E+20	601	713	42.0	50.0
RA14	0	270	623	79.8	88.7
RFA14	0	314	637	77.0	88.2
RFA24	0	311	644	73.8	83.7
RFS11	1E+20	575	696	22.2	29.1
RFS14	0	380	636	44.8	51.6

RFS21	1E+20	600	720	22.6	31.4
RFS24	0	400	642	43.2	46.6
RFS25	1E+20	635	713	19.9	28.0
RFS31	1E+21	654	740	15.9	20.2
RFS45	1E+21	678	735	16.3	22.0
RTA14	0	336	608	69.4	79.6
RTA24	0	329	618	76.4	86.7
RTS21	1E+20	599	740	33.2	47.6
RTS23	1E+20	597	722	31.0	40.9
RTS24	0	371	633	58.4	66.4
RTS31	1E+21	662	761	24.0	31.9
RTS33	1E+21	605	696	14.2	19.0
RTS34	0	389	641	54.9	61.7
SA01	0	269	626	83.3	92.0
SA02	0	287	621	70.5	78.9
SA03	0	207	631	80.7	90.8
SA04	0	229	635	75.0	82.0
SA05	1E+20	588	733	55.2	63.9
SA07	1E+21	664	759	45.7	52.6
SA08	1E+21	637	786	43.9	51.6
SA11	1E+20	553	765	52.0	60.7
Z012	0	417	569	10.9	11.0
Z017	1E+20	576	655	3.7	9.8
Z018	1E+21	600	663	3.2	8.6
Z020	1E+20	576	652	3.9	12.6
Z049	1E+21	615	673	3.5	13.2
Z050	0	419	578	12.1	25.9
Z102	0	425	597	12.0	20.6
Z1051	0	371	524	13.7	28.9
Z1052	0	376	521	14.0	24.8
Z1053	0	376	521	14.0	22.2
Z1054	0	368	520	12.5	21.7
Z108	1E+20	588	661	3.5	11.4
Z109	0	425	565	4.6	4.6
Z111	1E+21	621	683	3.3	8.1
Z112	1E+20	585	666	3.5	8.7
Z113	1E+21	618	677	3.4	8.5
Z115	0	436	527	1.2	1.2
Z117	1E+21	573	627	3.8	14.4
Z118	1E+21	578	640	3.8	14.5
Z119	1E+20	544	621	4.5	17.0

Z120	0	400	554	12.6	22.8
Z121	1E+20	534	608	4.3	14.0
ZN09	1E+20	610	656	1.6	5.0
ZN11	1E+20	630	670	1.4	4.5
ZN12	0	475	582	6.6	7.7
ZN13	0	478	584	7.1	9.4
ZN14	1E+21	658	688	1.4	6.1
ZN16	1E+21	649	682	1.1	3.6
ZN17	0	480	594	4.5	4.5
ZN18	1E+20	628	653	0.4	0.5
ZN20	1E+20	637	679	1.1	2.9
ZN21	0	481	588	8.1	10.5
ZN22	1E+21	663	688	0.7	1.9
ZN23	1E+21	638	638	0.1	0.1
ZN33	1E+20	602	635	1.6	13.2
ZN34	1E+20	595	628	1.2	9.4
ZN36	0	461	557	6.7	14.4
ZN38	1E+21	632	649	0.9	13.0
ZNFB09	0	467	582	8.1	15.0
ZNFB10	0	469	587	7.7	13.6
ZNFB11	0	473	592	7.8	18.1
ZNFB12	0	470	588	7.6	16.0
ZNFB13	0	463	577	6.8	12.4
ZO06	0	485	592	6.7	9.4
ZO07	1E+20	633	681	1.3	4.9
ZO08	1E+20	631	669	1.2	2.5
ZO13	1E+21	667	703	1.2	4.8
ZO14	1E+21	645	690	1.3	3.8
ZO15	0	491	589	5.6	7.3
ZO17	1E+20	630	640	0.2	0.2
ZO18	0	474	500	0.4	0.4
ZO19	1E+20	623	666	0.5	0.5
ZO25	0	492	593	3.3	3.4
ZO27	1E+21	532	543	0.0	0.1
ZO28	1E+21	669	702	0.5	0.5
ZO33	1E+20	590	634	1.6	9.5
ZO34	1E+20	600	634	1.5	10.7
ZO35	1E+21	624	654	1.3	9.5
ZO38	0	446	554	8.3	16.5
ZOT02	0	480	603	6.7	9.5
ZOT04	0	463	578	6.7	11.9

ZOT05	0	475	598	7.5	14.0